Soil Biology and Biochemistry 184 (2023) 109108

Contents lists available at ScienceDirect

Soil Biology and Biochemistry

journal homepage: www.elsevier.com/locate/soilbio

The ^{15}N-Gas flux method for quantifying denitrification in soil: Current progress and future directions

Gianni Micucci [a,*], Fotis Sgouridis [b], Niall P. McNamara [c], Stefan Krause [a], Iseult Lynch [a], Felicity Roos [d], Reinhard Well [e], Sami Ullah [a,f]

[a]. School of Geography, Earth and Environmental Sciences, University of Birmingham, Edgbaston, B15 2TT, Birmingham, United Kingdom
[b]. School of Geographical Sciences, University of Bristol, BS8 1SS, Bristol, United Kingdom
[c]. UK Centre for Ecology & Hydrology, Lancaster Environment Centre, LA1 4AP, Lancaster, United Kingdom
[d]. UK National Trust, SN2 2NA, Swindon, United Kingdom
[e]. Thünen Institute of Climate-Smart Agriculture, Bundesallee 65, 38116, Braunschweig, Germany
[f]. Birmingham Institute of Forest Research, University of Birmingham, Birmingham, UK

ARTICLE INFO

Keywords:
Denitrification
^{15}N gas flux method
Nitrogen cycling
Nitrous oxide emission
Stable isotope tracing

ABSTRACT

Denitrification in soil is a challenging process to quantify under *in situ* conditions, which seriously hampers the ability to accurately close or balance the nitrogen budget of terrestrial ecosystems. The ^{15}N Gas Flux method is one of the best-suited techniques for *in situ* measurement of denitrification. Using a stable ^{15}N-NO_3^- tracer injected or applied on the surface of soil under a closed static chamber, this method enables the measurement of both N_2O and N_2 denitrification fluxes. Its main limitation is the poor sensitivity towards N_2 emissions, which is a common weakness of all denitrification measurement methods. We also have identified four assumptions upon which this technique relies to be accurate: 1) homogenous distribution of the tracer inside the confined soil volume, 2) absence of hybrid molecule forming processes, 3) quantitative recovery of produced denitrification products inside the flux chamber headspace (no diffusive losses) and 4) no stimulatory impact of nitrate tracer and water additions on the dynamics of the denitrification process. In this review, we revisit the principles of the ^{15}N Gas Flux method, explore its evolution through time and assess the impact of the four assumptions through literature compilation and simulation. Finally, we elaborate and discuss key technical aspects of this method to help the reader in understanding and optimally applying the ^{15}N Gas Flux method for the measurement of denitrification. To this end, a decision tree has been implemented at the end of this study.

The outcome of our review shows that in order to address the main limitation of the ^{15}N Gas Flux method (poor N_2 sensitivity), a hybrid approach using an artificial N_2-depleted atmosphere in addition to ^{15}N isotopic tracer is a promising lead, although only a few studies have used it so far (even less so in the field). In particular, we demonstrate here the existence of a threshold of 10% atmospheric N_2 concentration background below which the sensitivity increases significantly. We also show that the four assumptions mentioned above are unlikely to be fully met under field conditions. The non-homogenous distribution of the ^{15}N tracer in soil has been shown by various authors to cause a 25% underestimation of the rate of denitrification at maximum. Through simulation, we show here that the presence of hybrid molecules should have a moderate impact on total fluxes (N_2 or N_2O similarly) as long as they contribute for no more than 50% of the total emissions (at which point they cause a 12.5% overestimation). The underestimation of denitrification due to subsoil diffusion, which has been reported to be as high as 37%, remains a challenge to quantify. Finally, the impact of substrate isotopic tracer and water additions on a hypothetical stimulation of the denitrification process needs further validation. Overall, our findings show that this method still holds a substantial promise for a more accurate quantification of *in situ* denitrification whilst considering the recommended mitigation of the methodological weaknesses in future research.

* Corresponding author.
E-mail address: gvm962@student.bham.ac.uk (G. Micucci).

https://doi.org/10.1016/j.soilbio.2023.109108
Received 25 January 2023; Received in revised form 20 June 2023; Accepted 21 June 2023
Available online 22 June 2023

Table 1
Different existing ^{15}N techniques for denitrification measurement, as reviewed by Myrold (1990) with further refinements and references.

Technique	Principle	Pro	Cons	Further reference
Variations in natural ^{15}N abundance	Studying the isotopic composition of soil N products. The different reactions of the N cycle will slightly discriminate between ^{14}N and ^{15}N atoms.	Does not require expensive ^{15}N tracer Can discriminate origins of N_2O.	Sensitive to temperature changes and C additions. Different pathways of N transformations have their own isotopic signature, making interpretation difficult.	Zaman et al. (2021 see chapter 7), Lewicka-Szczebak et al. (2020b).
^{15}N-labelled fertilizers in mass balance studies	Classic mass balance approach but the use of ^{15}N isotopes allows for a better sensitivity.	Integrates biological activity over space and time. Can easily be adapted to large plots in the field.	Difficulties to budget accurately the different ^{15}N pools, to design proper boundaries when in field. The use of microplots is not so accurate in fields. Accumulation of additive errors.	Meyer et al. (1989).
$^{15}NO_3$ Isotope Dilution and N cycle process models	Application of ^{15}N-NO_3 tracer and following the NO_3 concentration and its ^{15}N abundance.	Integrative in time and space and in estimating rates of other N cycle processes.	Assumes that the rate of nitrification and denitrification are constant. If the previous hypothesis is not true, this method requires a more difficult algebraic model. Only consider denitrification as NO_3 transformation and thus does not take in account immobilization, leaching, plant uptake and DNRA.	Müller et al. (2014).
Direct measurements of $^{15}N_2$ and $^{15}N_2O$ evolution	^{15}NGF method and alternative versions.	See this study.	See this study.	See this study.
^{15}N isotopic dilution	Creating a ^{15}N enriched atmosphere and monitor its dilution as denitrification occurs.	Less disruptive to the soil and easily moved from location to location in the field.	Assumes that rate of denitrification is constant and that no N_2 is fixed. Not a good sensitivity.	Yang et al. (2011) and Well and Butterbach-Bahl (2013) "Comments on Yang et al. study of (2011)".

1. Introduction

Denitrification is defined as the sequential reduction of soil nitrate (NO_3^-) through microbial respiration under anoxic or suboxic conditions. This nitrate is firstly transformed into nitrite (NO_2^-), then into gaseous nitric oxide (NO), gaseous nitrous oxide (N_2O) and finally into dinitrogen gas (N_2) through microbial redox reactions. In soil, denitrification is considered one of the major pathways of reactive nitrogen (N) removal, which is of particular importance for agricultural lands receiving large inputs of N fertilizer (Lassaletta. et al., 2014). The last intermediate of this sequential reaction is N_2O, which is a greenhouse gas 298 times more potent in inducing global warming than CO_2 over a 100-year period (IPCC, 2013); and which is also involved in the depletion of the ozone layer (Ravishankara et al., 2009). Denitrification has the ambiguous role of being both the only natural sink for respiratory reduction of N_2O into N_2 and a source of N_2O itself through incomplete denitrification. It is thus of primary importance to fully characterize this process and in particular the last step of the sequence, the reduction of N_2O into N_2. However, several difficulties have prevented scientists from accurately measuring denitrification for more than a century now (Almaraz et al., 2020). First, the large temporal and spatial variabilities of this process render it difficult to measure, and then model, global soil denitrification rates (Groffman and Tiedje, 1989; Seitzinger et al., 2006). Secondly, *in situ* measurements are hampered by technical complications; the biggest of which being undoubtedly the quantification of small N_2 denitrification fluxes against the high atmospheric N_2 background. Scientists have been working on developing methods to overcome this challenge and today, three techniques are mainly used to measure denitrification rates from soil (Well et al., 2019a); the ^{15}N Gas Flux method (^{15}NGF), the He/O_2 Gas Flow Soil Core method (He/O_2 GFSC) and the Acetylene Inhibition Technique (AIT). The ^{15}NGF uses a stable isotopic tracer ($^{15}NO_3^-$) to quantify denitrification by monitoring the ^{15}N signature of the soil-evolved N_2 (and N_2O) using Isotope Ratio Mass Spectrometry (IRMS). The He/O_2 GFSC uses a gas-tight incubation system under laboratory conditions to remove atmospheric N_2 so that the soil-evolved N_2 can be measured via gas chromatography (GC). Finally, the AIT is an indirect method of measurement which uses gaseous acetylene (C_2H_2) to block the N_2O reductase enzyme of denitrifier microbes, preventing them from reducing N_2O into N_2. Total denitrification is then determined by measuring N_2O emissions. This last technique has been widely used because of its simplicity and low cost, however, it has now become unpopular due to several limitations (Saggar et al., 2013). In particular, it has been shown that acetylene catalyses the oxidation of NO, causing a "scavenging" of NO and thus inhibiting the sequence of denitrification (Bollmann and Conrad, 1997; Nadeem et al., 2013). Furthermore, acetylene has an inhibitory effect on nitrification (which converts NH_4^+ into NO_3^-), leading to a decrease of the denitrification substrate in soil (Seitzinger et al., 1993). Finally, it has been shown that acetylene only partially inhibits the reduction of N_2O to N_2 (Simarmata et al., 1993; Yu et al., 2010). Overall, the use of the AIT leads to an unpredictable underestimation of denitrification. Laboratory studies (Yu et al., 2010) as well as field studies (Sgouridis et al., 2016) compared the AIT to ^{15}N tracer techniques and found significantly lower denitrification rates when using the AIT. The He/O_2 GFSC offers accurate measurements (Butterbach-Bahl et al., 2002; Cárdenas et al., 2003; Wang et al., 2013; Loick et al., 2016), but its need for a sophisticated gas-tight incubation system limits its use to laboratory studies only. The sensitivity of this method is also generally low and depends on the ability to reduce the atmospheric N_2 concentration (Friedl et al., 2020). Denitrification being complexly linked to its microenvironment, it is highly desirable to measure it *in situ*; and the ^{15}NGF is considered today the most viable method for this. Nonetheless, it also has key limitations and relies on certain assumptions that cannot always be met, tested or validated; inevitably causing biases in the estimation of denitrification. In particular, we identified the poor sensitivity towards N_2 emissions due to the very high atmospheric N_2 background as being the main limitation of this technique. Similarly, we identified four main assumptions upon which this method relies: 1) homogenous distribution of the label in soil leading to the formation of a single isotopic pool in equilibrium, 2) absence of hybrid molecule forming processes, 3) quantitative recovery of produced denitrification products in the flux chamber (no diffusive losses) and 4) no stimulatory impacts of tracer and water additions on the dynamics of the denitrification process. These assumptions are explained and detailed in this review and are in

good accordance with those identified in the recent study of Friedl et al. (2020). The other limitations identified by Friedl et al. (2020) are included in the technical challenges of this study (part 4). The ^{15}NGF is not the only existing ^{15}N tracer technique for the measurement of denitrification, Myrold (1990) made a review about all the existing ones (which are summed up in Table 1 along with analytical improvements and developments in recent years). However, the ^{15}NGF is currently the most widely used one for application in soil. It is thus important to revisit its history and explain its fundamental concepts, key hypotheses, further refinements over time and its accuracy in light of assumptions and recent advances in measurements under field conditions, which is the purpose of this study. Furthermore, this study suggests further directions via which to address the main limitations of the ^{15}NGF and fine-tune it for more accurate and robust measurements. Such an approach is imperative to resolve the enigma of accurate quantification of denitrification in soil.

1.1. Evolution of the ^{15}NGF

The use of a ^{15}N stable isotopic tracer for studying N transformations in soil started in the middle of the 1950's (Wijler and Delwiche, 1954; Hauck and Melsted, 1956). In particular, Hauck and Melsted (1956) added a ^{15}N-enriched nitrate solution to soil incubated under laboratory conditions. As this enriched nitrate was denitrified, gaseous ^{15}N-labelled N_2 was emitted and mixed with atmospheric N_2 (present at natural ^{15}N abundance ~0.37%). Hauck et al. (1958) used these data to show that the isotopic rate of exchange between ^{15}N and ^{14}N atoms was too slow to generate an isotopic equilibrium between the atmospheric and denitrifying pools. In other words, emitted and atmospheric N_2 molecules don't exchange ^{15}N isotopes at an appreciable rate, preventing the formation of a single isotopic pool in equilibrium (see part 2 of this study for further details). Using this property, it was possible to quantify the fluxes of denitrification and thus, the ^{15}NGF method was created (Hauck et al., 1958; Hauck and Bouldin, 1961). However, this technique was not popular at that time for several reasons. Firstly, compared to other ^{15}N tracer techniques (see Table 1), it requires large amounts of expensive and highly labelled tracer as well as complex gas handling and mass spectrometric techniques (Arah et al., 1993). Inversely, the AIT approach being cheaper and easier to use was preferred and saw an explosion of its use in the 1970's (Myrold, 1990). The unpopularity of the ^{15}NGF at that time can also be explained by the fact that triple collector IRMS, which can measure two ratios at the same time (contrarily to a double-collector IRMS), were only commercially available in the 1980's (Mulvaney, 1984). Triple collector IRMS are particularly convenient to study denitrification since N_2 and N_2O both require two measured ratios (see part 2.2 of this study). Finally, further studies were necessary to fully develop this method.

In the 1980's and 1990's, the ^{15}NGF saw a renewed interest thanks to numerous experimental and theoretical publications. It began with the work of Siegel et al. (1982) who reported a detection limit of 5 g N_2-N ha^{-1} day^{-1} using highly enriched ^{15}N label and newer mass spectrometers, where previous studies reported a detection limit from 100 to 1 000 g N_2-N ha^{-1} day^{-1} (Myrold, 1990; citing Focht and Stolzy, 1978; Rolston et al., 1978; Rolston et al., 1982). At the same time, Mulvaney and Kurtz (1982) presented a new method that enabled the measurement of N_2O production with the ^{15}NGF. It was then possible to estimate simultaneously fluxes of N_2 and N_2O using a single method, which was of great convenience. At this point, the theory of the ^{15}NGF was also investigated more deeply. New equations were derived by Mulvaney (1984) and further refined by Mulvaney and Boast (1986) to quantify denitrification. In 1988, a four-part series of articles critically evaluated the theory and assumptions of the ^{15}NGF method, especially the hypothesis that soil forms a sole isotopic pool after tracer injection (Boast et al., 1988; Vanden Heuvel et al., 1988; Mulvaney, 1988 and Mulvaney and Vanden Heuvel, 1988; see part 3.1 of this study for further details). It was followed by the work of Arah (1992) who derived new equations to measure denitrification rates and then proposed a model for apportioning the sources of N_2O using the ^{15}NGF method (Arah, 1997; see part 2.3 of this study). This model was later used and refined by Bergsma et al. (2001). Finally, it is worth mentioning that Laughlin and Stevens (2003) proved that ^{15}N labelled N_2 and N_2O could be stored in 12 mL Extainer® vials (Labco Ltd, U.K.) without any change of the ^{15}N enrichment. They even developed a model to account for diffusive losses, enabling a safe storage for 50 weeks. All this progress explains why the ^{15}NGF has increasingly become more popular at the start of the 2000's up to now (Stevens et al., 1997; Clough et al., 2001; Stevens and Laughlin 2002; Laughlin and Stevens 2002; Ruser et al., 2006; Cuhel et al., 2010; Baily et al., 2012; McGeough et al., 2012; Sgouridis and Ullah, 2015; Buchen et al., 2016; Krause et al., 2017; Deppe et al., 2017; Liu et al., 2022; amongst others).

The latest and most promising progress for the ^{15}NGF, is surely the use of a hybrid method. Indeed, as will be shown later in this study (part 4.2), the use of isotopes alone does not always guarantee a detection of denitrification fluxes. Thus, some studies have tried combining the ^{15}NGF method with the He/O_2 GFSC. The aim is to use ^{15}N isotopes under a N_2-depleted atmosphere, which highly increases the limit of detection. Early work of Spott et al. (2006) reported a detection limit of 4 μg N_2-N m^{-2} h^{-1} or (0.96 g N_2-N ha^{-1} day^{-1}). Although more expensive and more difficult to use, a small number of studies have used this hybrid method in the laboratory (Meyer et al., 2010; Scheer et al., 2016; Lewicka-Szczebak et al., 2017; Lewicka-Szczebak and Well, 2020a; Kemmann et al., 2021).

Recently, Well et al. (2019a) and Buchen-Tschiskale et al. (2023) brought this hybrid technique to the field and successfully measured denitrification with a sensitivity as low as 0.5 g N-(N_2+N_2O) ha^{-1} day^{-1}.

Other recent progresses on the ^{15}NGF include a simulation designed to account for diffusive losses (Well et al., 2019b; see part 3.3 of this study) and an evaluation of different tracer addition approaches (Lewicka-Szczebak and Well, 2020a) for both *in situ* and laboratory measurements.

Denitrification is still challenging to measure currently but after almost 70 years of development, the ^{15}NGF remains the most robust technique for its evaluation *in situ*.

2. Theory of the ^{15}NGF

The principle of the ^{15}NGF consists of applying a $^{15}NO_3^-$ tracer into soil incubated under a gas tight vessel and measuring the abundance of ^{15}N atoms in both denitrified N_2 and N_2O inside the headspace of the vessel. For *in situ* measurements, a chamber is usually fitted over a collar of confined ^{15}N-labelled soil volume. Laboratory incubations typically take place in sealed jars. Because of the already present N_2 and N_2O molecules in the atmosphere (with their natural ^{15}N abundance), equations had to be derived to discriminate the emitted fluxes of nitrogen (either N_2 or N_2O).

2.1. Isotopic equilibrium of the pools

We will only study the case of N_2 to illustrate the concept of pool at isotopic equilibrium here (but similar relations exist for N_2O). In the studied system, there are two pools contributing to the mix of N_2 molecules, the atmosphere where the molecules have a natural ^{15}N abundance ($\boldsymbol{a_a} \approx 0.37\%$) and the emitted molecules from the soil denitrifying pool. The denitrifying pool emits N_2 molecules with a ^{15}N abundance ($\boldsymbol{a_p}$) that depends on the enrichment level and quantity of tracer injected. When a pool is at isotopic equilibrium, the distribution of an isotope ^{Y}X within the molecules of this pool will follow a binomial law according to the abundance $\boldsymbol{a_p}$ of this isotope in the considered pool. This means that the probability to find $\boldsymbol{k}$ ^{Y}X isotopes in the $\boldsymbol{n}$ atoms of X inside a molecule equals:

$$p([{}^{Y}X]) = \binom{n}{k} a_p{}^{k}(1-a_p)^{n-k} \quad [1a]$$

$$a_p = \frac{number\ of\ isotopes\ {}^{Y}X\ \ present\ in\ the\ pool}{total\ number\ of\ atoms\ X\ in\ the\ pool} \quad [1b]$$

where $[{}^{Y}X]$ is the number of ^{Y}X isotopes inside a molecule containing n atoms of X.

In particular, for N_2 containing two N atoms, a pool with a ^{15}N abundance a_p will have the following distribution of isotopologues (molecules with same atomic identity but different isotope composition):

$$\%^{28}N_2 = (1-a_p)^2 \quad [2a]$$

$$\%^{29}N_2 = 2 \times a_p \times (1-a_p) \quad [2b]$$

$$\%^{30}N_2 = (a_p)^2 \quad [2c]$$

For example, considering that after tracer addition the incubated soil is at isotopic equilibrium and has an abundance $a_p = 20\%$ of ^{15}N atoms, the distribution will be 64%, 32% and 4% of $^{28}N_2$, $^{29}N_2$ and $^{30}N_2$ respectively. This ideal distribution assumes that no isotopic discrimination occurs during production of N_2O and its reduction to N_2. In theory, this hypothesis is not true due to equilibrium and kinetic isotope effects. Indeed, lightest atoms tend to react faster and thus, ^{14}N atoms will react preferentially, inducing a discrimination (also called isotopic fractionation) in favour of the lightest isotopologue ($^{28}N_2$). However, the ideal distribution is experimentally a good approximation (Cho and Sakdinan, 1978) especially when using highly enriched ^{15}N nitrate.

2.2. Equations for N_2 flux determination

Since Hauck et al. (1958) demonstrated that no isotopic exchange occurs at an appreciable rate between atmospheric N_2 and emitted N_2, the mix is therefore in a non-equilibrium state with two pools of different isotopologue distributions. Knowing these distributions, two main sets of equations were derived as shown below:

2.2.1. The Mulvaney & Boast model

This model was clearly established for both double and triple collector IRMS by Mulvaney (1984) with some mathematical approximations. It was later refined by Mulvaney and Boast (1986) without any approximations. Although it was shown that the simplified equations only induce a significant error when the tracer enrichment in the soil is lower than 20%, only the model without simplification will be considered here. These equations are based on the work of Hauck and Bouldin (1961) and use the differences of the R29 and R30 ratios of N_2 before and after soil incubation following ^{15}N tracer addition. For an IRMS with a triple collector, R29 is the ratio of $^{29}N_2$ to $^{28}N_2$ and R30 is the ratio of $^{30}N_2$ to $^{28}N_2$. Hence:

$$R29_0 = \frac{{}^{29}N_{2\ atmosphere}}{{}^{28}N_{2\ atmosphere}}\ (before\ incubation) \quad [3a]$$

$$R29_t = \frac{{}^{29}N_{2\ atmosphere} + {}^{29}N_{2\ denitrified}}{{}^{28}N_{2\ atmosphere} + {}^{28}N_{2\ denitrified}}\ (after\ incubation) \quad [3b]$$

$$\Delta R29 = R29_t - R29_0 \quad [3c]$$

Dividing the top and bottom parts of the $R29_t$ ratio by the total amount of N_2 and using the above-mentioned distribution of isotopologues (equations [2a] to [2c]) enable to rewrite $R29_t$ as:

$$R29_t = \frac{(1-d)(\%^{29}N_{2\ atmosphere}) + d(\%^{29}N_{2\ denitrified})}{(1-d)(\%^{28}N_{2\ atmosphere}) + d(\%^{28}N_{2\ denitrified})} \quad [3d]$$

$$R29_t = \frac{(1-d)[2a_a(1-a_a)] + d[2a_p(1-a_p)]}{(1-d)(1-a_a)^2 + d(1-a_p)^2} \quad [3e]$$

where d is the proportion of N_2 that derives from denitrification,

$$d = \frac{N_2\ denitrified}{N_2\ denitrified + N_2\ atmosphere} \quad [3f]$$

Similar equations exist for R30.

Note that a_p and a_a have been used here for the ^{15}N abundance of the soil denitrifying pool and of the atmosphere respectively, rather than $^{15}X_N$ and γ as in Mulvaney and Boast (1986) to keep a consistent nomenclature.

The authors then isolate a_p from these equations to determine d with the following equations:

$$a_p = \frac{-B + \sqrt{B^2 - 4AC}}{2A} \quad [3g]$$

where,

$$A = 1 - 2a_a + 2(1-a_a)\frac{\Delta R30}{\Delta R29} \quad [3h]$$

$$B = 2a_a{}^2 - 2(1-a_a{}^2)\frac{\Delta R30}{\Delta R29} \quad [3i]$$

$$C = 2a_a(1-a_a)\frac{\Delta R30}{\Delta R29} - a_a{}^2 \quad [3j]$$

And finally,

$$d = \frac{\Delta R29(1-a_a)^2}{\frac{2(1-a_p)(a_p-a_a)}{(1-a_a)} + \Delta R29(1-a_a)^2 - \Delta R29(1-a_p)^2} \quad [3k]$$

Technically, the ratio d is defined for a number of molecules (in mol), but under the headspace of an incubation vessel of constant volume, it is possible to express the concentration of soil-evolved N_2 by:

$$[N_2]_{denitrified} = \frac{d}{1-d}[N_2]_{atm} \quad [3l]$$

where, $[N_2]_{denitrified}$ is the concentration of denitrified N_2 (ppm), $[N_2]_{atm}$ is the concentration of atmospheric N_2 (ppm).

This concentration is also given by:

$$[N_2]_{denitrified} = d[N_2]_{total} \quad [3m]$$

where, $[N_2]_{total}$ is the total concentration of N_2 after incubation (denitrified + atmosphere, in ppm).

Since the total N_2 concentration does not vary significantly after denitrification (typically $10^{-8} < d < 10^{-4}$), some authors have also calculated the quantity of evolved N_2 as:

$$[N_2]_{denitrified} = d[N_2]_{atm} \quad [3n]$$

which is a good approximation to the result given with equation [3l] since $(1-d) \approx 1$.

2.2.2. The Arah model

A second set of equations has been derived by Arah (1992). These equations are based on a mixing model of the ^{15}N pools (denitrified and atmospheric) rather than a difference before and after incubation. These equations have been rewritten by Russow et al. (1996) and later by Spott et al. (2006). The latter version is the most commonly used and is the one presented here.

Again, soil is incubated in an isolation vessel which encloses the native atmosphere inside it. Initially, the ^{15}N abundance in the headspace of the vessel is the natural ^{15}N abundance a_a. After the duration of the incubation, it will change due to the denitrification of the soil ^{15}N-

Table 2
Simulation of a mix between atmospheric and denitrified N_2.

Atmosphere						
Number of molecules	a_a	$^{28}N_2$	$^{29}N_2$	$^{30}N_2$		
8.39E+22	0.3663%	8.33E+22	6.13E+20	1.13E+18		
Denitrification						
Number of molecules	a_p	$^{28}N_2$	$^{29}N_2$	$^{30}N_2$		
4.20E+18	50%	1.05E+18	2.1E+18	1.05E+18		
Mix						
$^{28}N_2$	$^{29}N_2$	$^{30}N_2$	$R29_{(0)}$	$R29_t$	$R30_{(0)}$	$R30_t$
8.33E+22	6.15E+20	2.18E+18	7.35E-03	7.38E-03	1.35E-05	2.61E-05
Mulvaney & Boast						
ΔR29	ΔR30	A	B	C	$^{15}X_N\ (a_p)$	d
2.51E-05	1.26E-05	1.99	−1.00	3.65E-03	50%	5.00E-05
Arah						
a_m	α_m	a_p	d			
3.69E-03	2.59E-05	50%	5.00E-05			

Simulation of a 4L chamber, considering isotopic equilibrium of atmospheric and soil denitrifying pools, as well as atmospheric pressure inside the chamber and the ideal gas law. A coefficient d equal to 5.10^{-5} has been set for this simulation. The "Atmosphere" and "Denitrification" lines at the top contain the data used for the simulation. Mulvaney and Boast (1986) and Arah (1992) models both yielded the correct results. This simulation also enables to better apprehend the difference in order of magnitude between the quantities of denitrified and atmospheric N_2. See parts 2.2.1 and 2.2.2 of this study for explanations of the calculated coefficients.

NO_3^- to a new abundance a_m, given by:

$$a_m = (1-d) \times a_a + d \times a_p \quad [4a]$$

where we denote again a_p to be the enrichment of the soil denitrifying pool while d is still the proportion of N_2 that derives from denitrification (see equation [3f]). a_m and a_a can be calculated as:

$$a_m = \frac{R_{29} + 2R_{30}}{2(1 + R_{29} + R_{30})} \ (after\ incubation) \quad [4b]$$

$$a_a = \frac{R_{29} + 2R_{30}}{2(1 + R_{29} + R_{30})} \ (before\ incubation) \quad [4c]$$

The same mixing equation can be used for the proportion of $^{30}N_2$. Let us call α_i the proportion of $^{30}N_2$ (see equation [2c]) in the pool i:

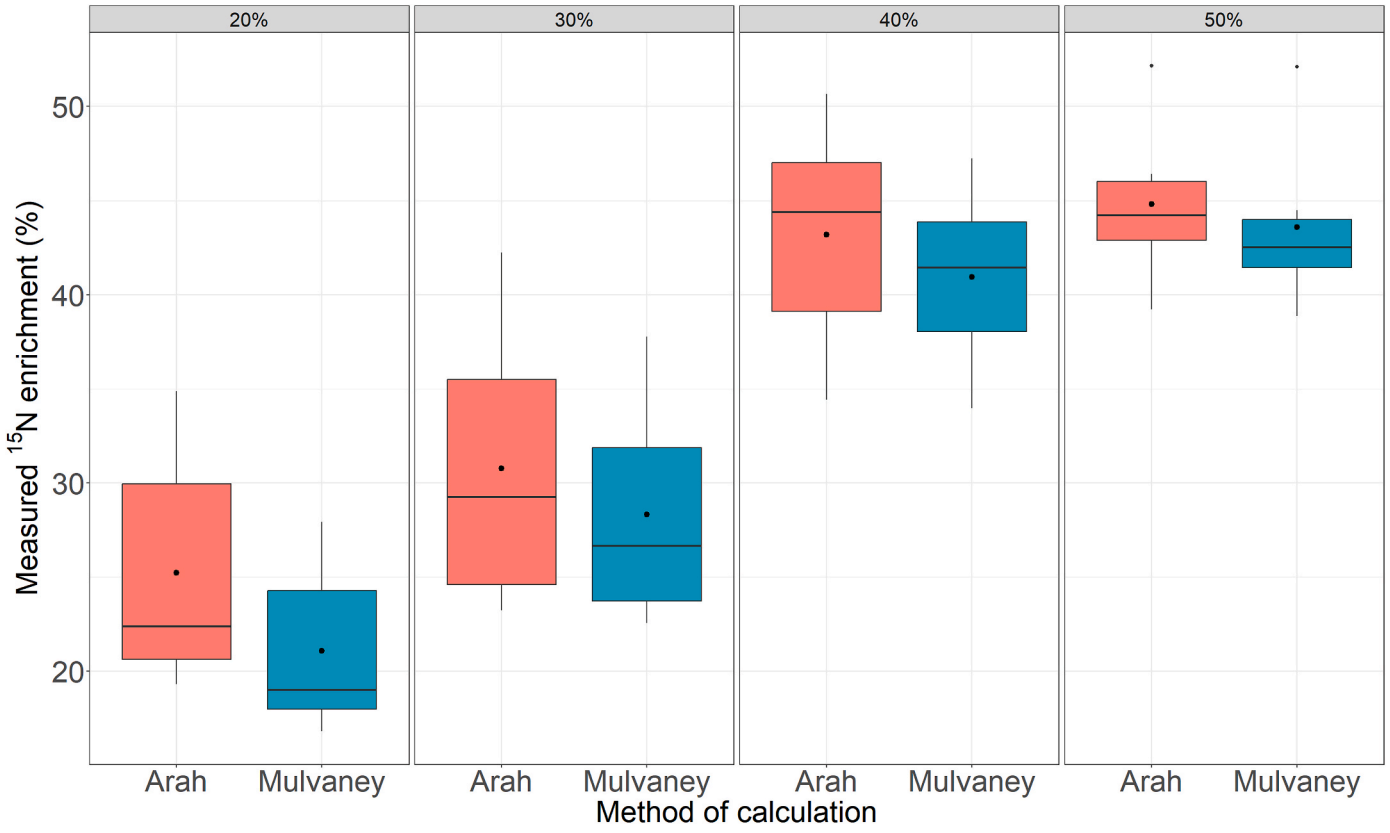

Fig. 1. Measured ^{15}N enrichment of the soil denitrifying pool for different ^{15}N enrichment targets (20, 30, 40 or 50%), calculated using either the Arah (red) or Mulvaney & Boast (blue) equations during one of our laboratory experiments (unpublished results). The mean of each series is represented by a large point in the middle of the associated box.

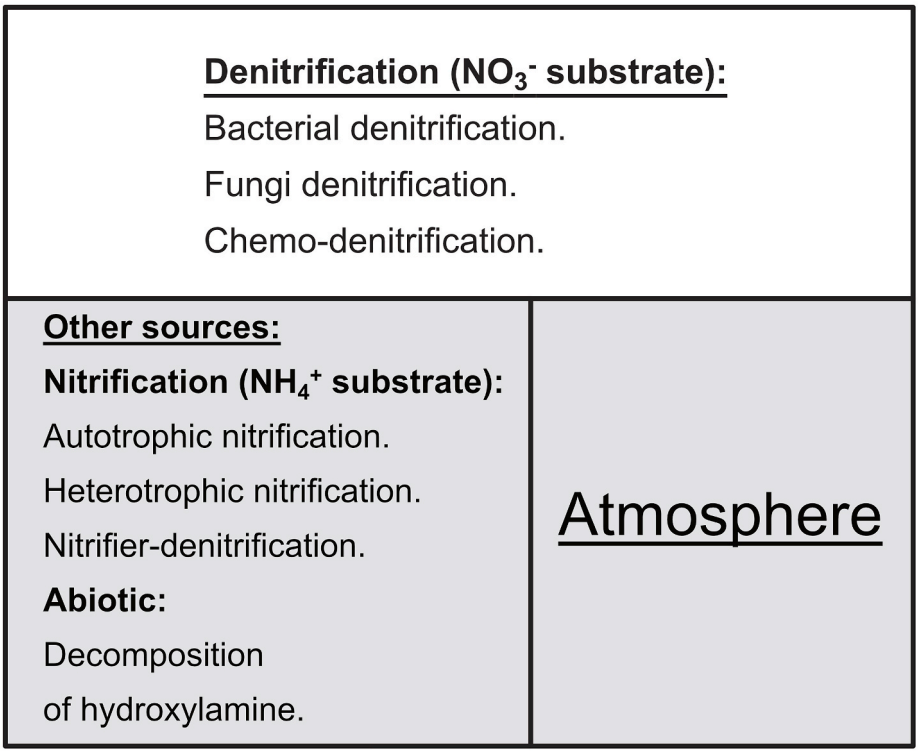

Fig. 2. Composition of total N_2O after incubation. The labelling of the nitrate pool enables the contribution of the denitrification sources (white box) to be determined against the other sources of N_2O (grey boxes).

$$\alpha_m = (1-d) \times \alpha_a + d \times \alpha_p \quad [4d]$$

Where $\boldsymbol{i}$ has been replaced with:

- m for the mix (atmospheric N_2 + denitrified N_2).
- a for the atmospheric pool.
- p for the denitrifying pool.

One can calculate $\boldsymbol{\alpha_m}$ as:

$$\alpha_m = \frac{R_{30}}{1 + R_{29} + R_{30}} \ (after\ incubation) \quad [4e]$$

Using the binomial distribution, the authors isolate quantities $\boldsymbol{a_p}$ and $\boldsymbol{d}$ by:

$$a_p = \frac{\alpha_m - a_a a_m}{a_m - a_a} \quad [4f]$$

$$d = \frac{a_m - a_a}{a_p - a_a} \quad [4g]$$

The concentration of evolved N_2 inside the incubation vessel is then calculated similarly to the model of Mulvaney & Boast (equations [3l] to [3n]).

2.2.3. Discussion and further refinements

Theoretically, both systems of equations are valid. They indeed give the same and correct results when simulating a mix of two pools at isotopic equilibrium. This can be seen in Table 2 which simulates a mix of atmospheric N_2 and denitrified N_2 in a 4 L chamber, considering atmospheric pressure and assuming ideal gas law. However, different results will be obtained depending on which model is used on real experimental data. It is difficult to predict *a priori* which system will be the most accurate. During one of our laboratory incubations (unpublished data), we compared both models of calculation on N_2O emissions (which can also be calculated via the two models but for which sensitivity is higher, see part 2.3 of this study). The experiment consisted of adding different amounts of $^{15}NO_3^-$ tracer to the same soil mix to target a 20, 30, 40 or 50% ^{15}N enrichment of the soil denitrifying pool. Fig. 1 shows boxplots of the observed enrichments for each treatment (6 replica, 6 h of incubation) calculated using the two sets of equations.

It can be seen from Fig. 1 that using the same raw data, the two systems of calculation yielded different results. Paired student-t tests for each enrichment showed that these systems were statistically different. It is also interesting to note that in exactly each case, the calculated ^{15}N enrichment with the Arah model was strictly superior to the one calculated with the Mulvaney & Boast model. After 24 h, the two models were very comparable, with the Arah model being on average only 2.22% higher. But overall, the Mulvaney & Boast model seems to be closer to the targeted enrichment and to have a smaller variability (full study to be published). Ideally, further data would be needed to confirm this trend.

It can also be noted that R30 data are often below the limit of detection of the instrument and difficult to read (see parts 4.2 and 4.3 of this study), which makes both systems of calculation difficult to use. To solve this issue, Spott et al. (2006) derived an equation from the Arah model that solely uses R29 (after incubation) data. Thus, $\boldsymbol{d}$ can be calculated as:

$$d = \frac{1}{1 - \frac{R29\left(1-a_p\right)^2 - 2a_p\left(1-a_p\right)}{R29(1-a_a)^2 - 2a_a(1-a_a)}} \quad [5a]$$

This equation is a rewritten version of equation [3k] from the Mulvaney and Boast (1986) model. However, it requires the user to know the degree of enrichment of the soil denitrifying pool $\boldsymbol{a_p}$ which cannot be determined with R29 data alone. A useful tip is to use the enrichment calculated from the N_2O data (see part 2.3 of this study) and hypothesize that N_2O and N_2 have the same degree of ^{15}N enrichment. This is a reasonable assumption since they both originate from the same denitrifying pool, but it could be biased due to heterogeneity of ^{15}N label application and denitrification dynamics (Zaman et al., 2021, chapter

7.2.6.2). However, the isotopic data for N_2O are usually much easier to read since the atmospheric background of N_2O is considerably lower (~0.330 ppm_v, part per million volumetric). In some cases, if the N_2O data cannot be used either (e.g. low N_2O emissions), it is possible to estimate the ^{15}N enrichment of the soil denitrifying pool $\boldsymbol{a_p}$ by measuring the ^{15}N enrichment of the soil nitrate $\boldsymbol{a_{NO3}}$ (as in Kulkarni et al., 2014). In theory, $\boldsymbol{a_p}$ and $\boldsymbol{a_{NO3}}$ should be similar, but this is generally not the case due to the dynamics of denitrification in soil, heterogeneity of the label application and dilution of the label by nitrification (Buchen et al., 2016; Deppe et al., 2017; Lewicka-Szczebak and Well, 2020a; Friedl et al., 2020; Zaman et al., 2021, chapter 7.2.6.2). This is why $\boldsymbol{a_p}$ is more generally referred as the "^{15}N enrichment of the NO_3^- pool undergoing denitrification" and why it needs to be recalculated before the coefficient $\boldsymbol{d}$.

Although the atmospheric R29 and R30 ratios are supposedly constant, it is recommended to make measurements at t = 0 for improved accuracy. Thus, for the model of Mulvaney and Boast (1986), it is probably best to recalculate the ^{15}N abundance of atmosphere $\boldsymbol{a_a}$ just as in the model of Arah (equation [4c]) rather than using the average natural ^{15}N abundance:

$$a_a = \frac{R_{29} + 2R_{30}}{2(1 + R_{29} + R_{30})} \quad (t = 0) \qquad [5b]$$

In the case of the Spott et al. (2006) equation using only R29 (equation [5a]), one can recalculate the atmospheric ^{15}N abundance $\boldsymbol{a_a}$ as:

$$a_a = \frac{R_{29}}{2 + R_{29}} \quad (t = 0) \qquad [5c]$$

Finally, the two-pool model can be biased if other sources of N_2 production are present. If a third source comes from an unlabelled soil pool and is at isotopic equilibrium, then this dinitrogen is produced at natural ^{15}N abundance with the same isotopologue distribution as the atmospheric N_2. Hence, a two-pool model is still applicable considering that one of the two pools is the sum of (atmosphere + third source).

The production of hybrid N_2 could however bias the calculations as shown in section 3.2.

2.3. Methods for determination of N_2O

The total concentration of N_2O can be monitored with GC measurements however, the complementary use of the ^{15}NGF enables measurement of the purely denitrified N_2O contribution, allowing for source partitioning. If hybrid processes are omitted (see part 3.2), the composition of total measured N_2O after incubation can be represented as shown in Fig. 2 (Bremner, 1997; Wrage et al., 2001; Zou et al., 2014).

The concentration of atmospheric N_2O is assumed to stay constant during the incubation and is given by a GC measurement at t = 0 (although it can theoretically be reduced to N_2 via denitrification).

The source partitioning with the use of the ^{15}NGF enables discrimination between nitrate-derived N_2O and the other sources (see Fig. 2). Nitrification is most likely the biggest of these additional sources of N_2O, thus we will distinguish "denitrification" and "nitrification" as sources of N_2O from soil for the labelled and unlabelled pools respectively (after subtraction of atmospheric N_2O). It can be added that theoretically, some of the ^{15}N tracer applied as nitrate can be transformed into ammonium through dissimilatory nitrate reduction to ammonium (DNRA) and then be emitted as N_2O through nitrification, thus biasing the source partitioning. This is however unlikely to cause a significant error during the course of an incubation experiment.

The measurement of denitrified N_2O enables quantification of two important parameters of denitrification, which are:

The proportion of emitted N_2O that originates from denitrification (source partitioning),

$$\%N_2O_{denitrified} = \frac{N_2O_{denitrified}}{N_2O_{emitted}} \qquad [6a]$$

and the proportion of denitrification products emitted as N_2O (product ratio),

$$R_{N2O} = \frac{N_2O_{denitrified}}{N_{2\ denitrified} + N_2O_{denitrified}} \qquad [6b]$$

These quantities are probably better characterized by using fluxes calculated from different time step measurements, rather than just the concentration after one time step. However, using multiple time steps for the ^{15}NGF can be rather expensive.

Using the ^{15}NGF method to measure denitrified N_2O allows the accurate determination of the product ratio (equation [6b]), since both N_2O and N_2 have been measured with the same technique. For example, if the denitrifying pool is not uniformly labelled, N_2 emissions will be underestimated (see part 3.1 of this study). Assuming that N_2O derives from the same soil mineral pool as N_2, the amount of emitted N_2O from denitrification will be underestimated in the same way and thus the denitrification product ratio will be determined more accurately (Bergsma et al., 2001). Furthermore, if the N_2O emitted by denitrification does derive from the same mineral pool as N_2, then it will have the same ^{15}N abundance (Arah, 1997). Using the ^{15}NGF for N_2O measurement then offers an independent determination of the soil ^{15}N abundance $\boldsymbol{a_p}$ (Bergsma et al., 2001) and is useful to determine N_2 flux without R30 data (see part 2.2.3 of this study). Partitioning the sources of N_2O is also possible by studying the position of naturally abundant ^{15}N isotopes in the N_2O molecules (Yoshida and Toyoda, 2000; Yu et al., 2020), however, more potential exists in the use of ^{15}N tracer (Stevens et al., 1997).

The first analyses of N_2O using ^{15}N isotopes were performed between the 1970's and the 1980's (Guiraud and Berlier, 1970; Cho and Sakdinan, 1978; Focht et al., 1979, 1980). The ^{15}N isotope was used to discriminate CO_2 from N_2O since they both have an atomic mass of 44. Thus, the determination of emitted N_2O was made from the measurements at m/z 45 and 46 (Cho and Sakdinan, 1978). However, mass spectrometers at that time were not really designed for measurements at those values and the presence of natural oxygen isotopes complicated the measurements both for CO_2 and N_2O (Mulvaney and Kurtz, 1982). Mulvaney and Kurtz (1982) developed another method involving the dilution of denitrified N_2O with a known amount of N_2 at natural ^{15}N abundance. They then reduced the N_2O gas into N_2, leading to a two-pool system easily resolved with the equations previously derived for N_2. Work from Stevens et al. (1993) represents the first attempt to directly quantify the amount of evolved N_2O through the ratios m/z = 44, 45, 46. Using an N_2O reference of known amount and isotopic composition, the authors were able to directly quantify the fluxes of denitrified N_2O. Later, both Stevens et al. (1997) and Arah (1997) developed models to measure the relative contributions of nitrification and denitrification to N_2O emissions. Stevens et al. (1997) labelled either the NO_3^- or NH_4^+ pool and then linked the ^{15}N abundance of these pools to the contributions of denitrification and nitrification respectively. On the other hand, Arah (1997) used the measured ^{15}N abundance from emitted N_2 and hypothesized that the denitrified N_2O evolves from the same mineral pool, having thus the same ^{15}N abundance. However, Arah (1997) states that emitted N_2O evolves in an atmosphere where its initial concentration is negligible. This is not totally true, as the concentration of atmospheric N_2O is approximately 0.330 ppm_v. Bergsma et al. (2001) succeeded to have sensitivity at both this low atmospheric level and at higher concentration and enrichment levels (after incubation following application of ^{15}N tracer) by modifying the head amplifier of their IRMS. By doing so, they developed a new model where N_2O emissions from denitrification can be measured similarly to the way N_2 emissions are measured. Concretely, the same equations as the ones presented in sections 2.2.1 and 2.2.2 can be applied if the ratios R29′ and R30' (where a prime has been used to

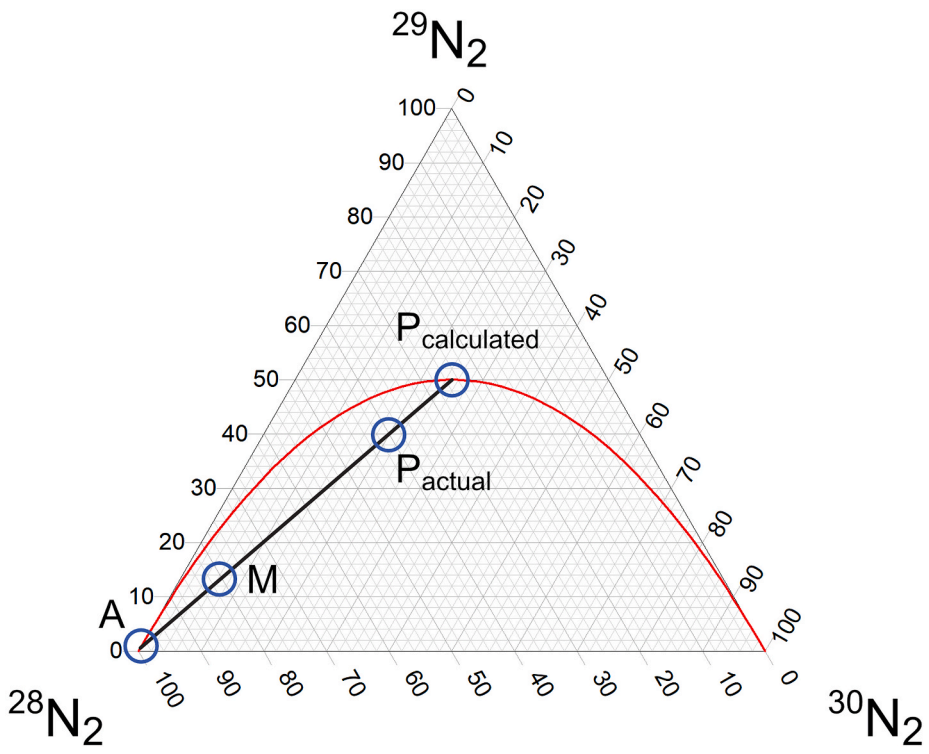

Fig. 3. Ternary diagram representation of the relative proportions of N_2 isotopologues in a mix between denitrification and atmosphere. Point A represents the atmospheric N_2. Point M is the mixture of atmospheric and denitrified N_2. Point $P_{calculated}$ represents the estimated isotopologue composition of the denitrifying pool following the isotopic equilibrium hypothesis. Point P_{actual} represents a more realistic isotopologue composition if we consider the soil denitrifying pool as the result of smaller sub-pools at isotopic equilibrium, due to the heterogeneity of soil and injected tracer distribution. Please note this is a schematic view for easier reading, in reality point M will be much closer to point A because of the large proportion of atmospheric N_2.

distinguish N_2O ratios) are modified to take oxygen isotopes into account:

$$R29' = R45 - R17 \quad [6c]$$

$$R30' = R46 - (R29)(R17) - R18 \quad [6d]$$

where R45 and R46 are the ratios ($^{45}N_2O/^{44}N_2O$) and ($^{46}N_2O/^{44}N_2O$) respectively, R17 is the $^{17}O/^{16}O$ ratio and R18 is the $^{18}O/^{16}O$ ratio. R17 and R18 are constant at natural abundance, Bergsma et al. (2001) used the values of 0.000373 and 0.0020052 respectively, based on the work of Hayes (1993).

The model of Bergsma et al. (2001) hypothesises that N_2O derived from nitrification has the same ^{15}N natural abundance as atmospheric N_2O. This transforms a three-pool model into a two-pool model, one of these two pools being the sum of (atmosphere + nitrification), as shown in Fig. 2. The equations presented in sections 2.2.1 or 2.2.2 enable the calculation of ***d'***, the fraction of total N_2O that derives from denitrification, similarly to how ***d*** is calculated for N_2 emissions. This coefficient then needs to be multiplied by the total amount (or concentration) of N_2O measured by GC.

$$[N_2O]_{denitrified} = d'[N_2O]_{total} \quad [6e]$$

where, $[N_2O]_{denitrified}$ is the concentration of denitrified N_2O (ppm) and $[N_2O]_{total}$ is the concentration of total N_2O (ppm) measured by GC.

The quantity (1-***d'***) is the sum of the contributions of atmosphere and nitrification. Nitrification can be determined as:

$$[N_2O]_{nitrification} = [N_2O]_{total} - [N_2O]_{denitrified} - [N_2O]_{atmosphere} \quad [6f]$$

where, $[N_2O]_{nitrification}$ is the concentration of nitrified N_2O (ppm) and $[N_2O]_{atmosphere}$ is the concentration of atmospheric N_2O (ppm), measured by GC at time 0.

The method of Bergsma et al. (2001) is probably to date, the best method for the evaluation of denitrified N_2O. Furthermore, modern IRMS have a higher range of sensitivity for N_2O analysis and modifying the amplification of the instrument is no longer necessary unless the sample is very concentrated (approx. 5 ppm of N_2O, as a general guidance). Similarly to the case of N_2, calculations can be biased if hybrid N_2O is produced, see section 3.2.

3. Assumptions of the ^{15}NGF method

We identified four assumptions upon which the ^{15}NGF relies to be accurate. These assumptions are:

1) The tracer is distributed homogenously in the confined soil leading to the formation of a single isotopic pool in equilibrium.
2) No hybrid molecules are formed during the incubation.
3) The denitrification products are recovered quantitatively in the flux chamber (no diffusive losses).
4) No stimulatory impacts of tracer and water additions on the dynamics of the denitrification process.

In the following section, we discuss how these different assumptions might cause under or over-estimation of the measured denitrifying flux and how we can mitigate their impact.

3.1. Homogenous distribution of the tracer in the soil

3.1.1. Spatial variations

The calculations of the ^{15}NGF are based on the hypothesis that the soil denitrifying pool of the incubated soil is at isotopic equilibrium. This is very unlikely since soil is highly heterogeneous and because it is virtually impossible to achieve a perfectly homogeneous application of tracer into the soil. For example, in their study of tracer distribution using Bromide (Br-), Berendt et al. (2020) found a theoretical $^{15}NO_3^-$ enrichment of 57–59 at% in the upper 2.5 cm and 26–57 at% in 5–10 cm when targeting a 60% enrichment using different application methods. Furthermore, denitrification presents a great spatial variability, occurring typically in anaerobic microsites of soil (Buchen et al., 2016).

Bergsma et al. (1999) used a ternary diagram to represent the distribution of N_2 isotopologues as can be seen in Fig. 3.

Each side of the triangle represents one of the isotopologues $^{28}N_2$,

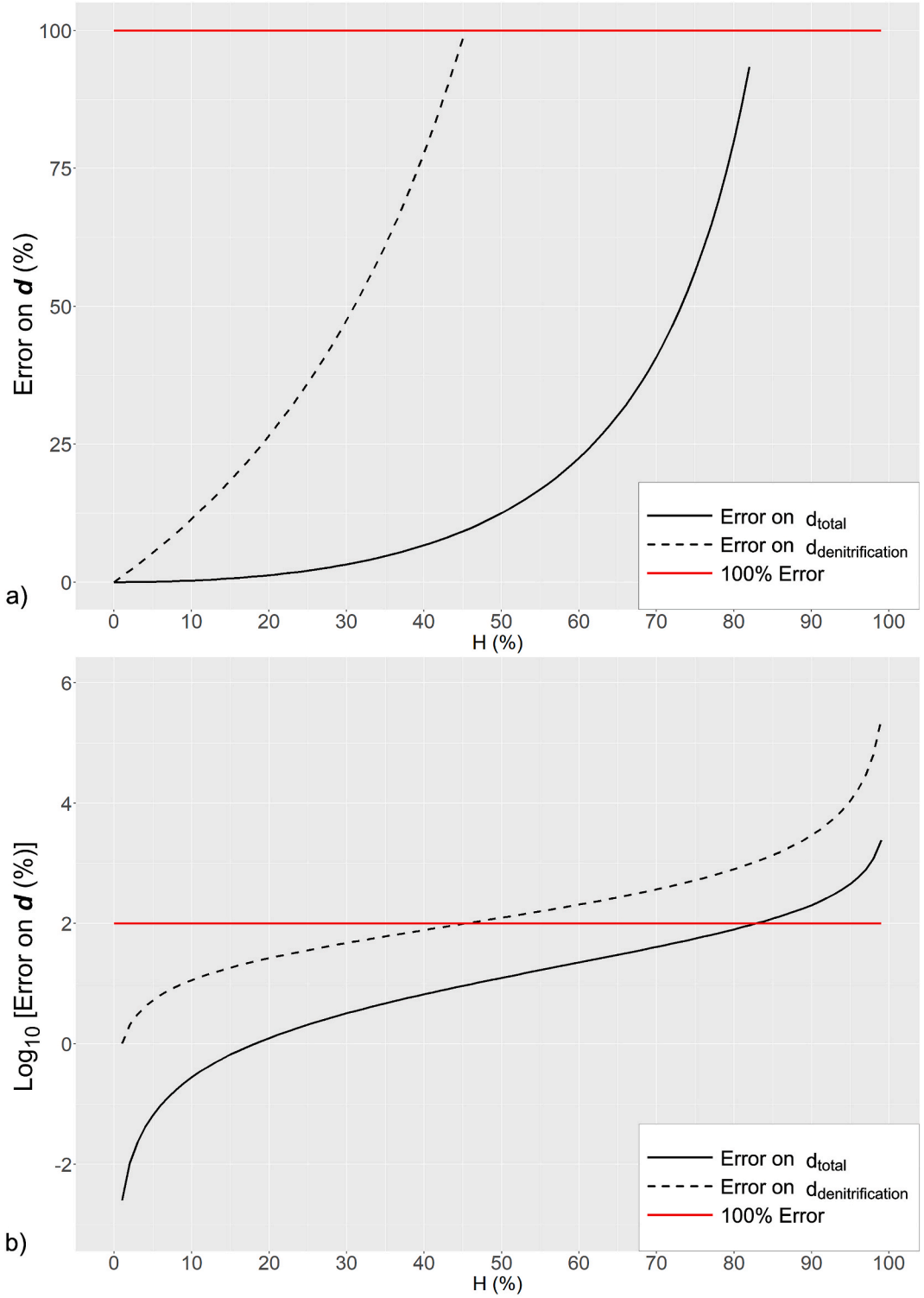

Fig. 4. (a) Evolution of the error made on the calculation of d_{total} (solid line) and $d_{dentrification}$ (dashed line) with H when ignoring the hybrid sources of denitrification, based on 396 simulated cases; (b) same evolution but represented in a logarithmic scale (log 10). The horizontal red line represents an error of 100%. The presence of hybrid molecules systematically causes an overestimation of all emitted molecules (d_{total}) and of molecules emitted through classic denitrification ($d_{dentrification}$). The magnitude of these overestimations does not depend on a_p nor d.

$^{29}N_2$ and $^{30}N_2$ and any point in the diagram is defined by its unique relative proportions of the three isotopologues. The red line represents isotopic equilibrium. Thus, any pool in such equilibrium is represented by a point on this curve that solely depends on its ^{15}N abundance. As Bergsma et al. (1999) explained, the two initial pools (A for atmosphere and P for soil) fall on the red curve. The mix (M) is a point that falls on the segment between A and P depending on the relative proportions of atmospheric and emitted N_2. The point M is necessarily below the equilibrium curve, as are all mixes of different pools at isotopic equilibrium (given that those pools have different ^{15}N abundances). In the same idea, the non-ideal soil denitrifying pool could be thought of as the result of different smaller sub-pools at isotopic equilibrium with various

^{15}N abundances, due to the heterogeneity of soil and injected tracer distribution. Then the actual distribution of isotopologues of the denitrified molecules would be represented by a point P_{actual} somewhere beneath the equilibrium curve and necessarily on the line (AM).

Now, when measurements are made, only the composition of atmosphere (A) and the mix (M) are determined. The hypothesis of isotopic equilibrium of the soil denitrifying pool infers that the point P belongs to the red curve ($P_{calculated}$), thus overestimating the real point P_{actual}, as shown in Fig. 3. The real proportion ***d*** of denitrified N_2 is determined by the ratio AM/AP_{actual} but the one actually calculated is given by $AM/AP_{calculated}$, causing a systematic underestimation.

Boast et al. (1988) and later Arah (1992) both modelled this system in a series of equations to prove that the ^{15}N abundance is always overestimated while the proportion ***d*** is always underestimated when multiple sub-pools exist. Through simulation, Vanden Heuvel et al. (1988) showed that larger errors arise when the range of enrichments of the sub-pools increases and when the number of pools decreases. This reflects the need to have a homogenous distribution of the tracer in the soil.

Through a series of simulations, Arah (1992) realised that overall, the fraction ***d*** seems to be underestimated by 24% independently of the magnitude of the flux when multiple sub-pools exist. This result has been confirmed independently by Bergsma et al. (1999) using a different model, where the range of the ^{15}N abundances of the sub-pools is distributed uniformly between all of these sub-pools. When using a range from natural abundance to any greater value, they found a systematic underestimation of 25%, which is very close to the result of Arah (1992).

The validity of these conclusions was tested in laboratory studies by Mulvaney (1988) who measured fluxes of N_2O emissions via either GC or the ^{15}NGF (after chemical reduction of total N_2O into N_2 for the ^{15}NGF, see Mulvaney and Kurtz, 1982). Firstly, a good correlation was observed between the two techniques when forming N_2O via chemical oxidation of ^{15}N-labelled NH_2OH/HCl. This means that the emitted N_2O existed as a sole isotopic pool. The same experiment but with two pools of different ^{15}N abundances confirmed that the quantity ***d*** is underestimated with the ^{15}NGF when multiple pools are present, but only significantly when there is a considerable difference in enrichment between the two pools. An underestimation of 10% was reported in this study using a pool enriched at 32% in ^{15}N atoms and one at 53%. Laboratory experiments on soil and soil slurries (to ensure a thorough mixing of the label) offered mixed results. Although the ^{15}NGF often underestimated the rate measured by GC, it also overestimated it in some cases. Mulvaney and Vanden Heuvel (1988) did the same experiment in the field and found similar results, i.e.; the ^{15}NGF often underestimated the N_2O concentration (by up to 33%) and overestimated it only sometimes (by up to 11%). According to the authors, the underestimations by more than 25% and the overestimations were explained by analytical errors and it was concluded that correct measurements can still be obtained even without perfect distribution of the ^{15}N label in the soil. It can be noted that Fig. 2 from Mulvaney and Vanden Heuvel (1988) offers a good visual representation of the spatial heterogeneity of the ^{15}N abundance in soil after tracer injection.

Stevens et al. (1997) also studied the impact of the non-homogenous ^{15}N label distribution on the isotopic equilibrium of the soil denitrifying pool by measuring N_2O emissions but used acetylene (C_2H_2) to block nitrification this time. The ^{15}N abundance of N_2O was then calculated via either R45 or R46 using a one-pool model and values were compared to see if they agreed. Good correlation was observed (Table 2 of the cited reference) which indicates again that the assumption of isotopic equilibrium of the soil denitrifying pool is experimentally a good approximation, even without perfect label distribution.

3.1.2. Temporal variations

As mentioned by Russow et al. (1996), mineralization and nitrification tend to modify the ^{15}N abundance of the soil denitrifying pool after injection of the tracer. Similarly to spatial heterogeneity, if the ^{15}N abundance of nitrate varies over time, the soil denitrifying pool cannot be considered at isotopic equilibrium. The temporal variations are however a bit different as they change the overall ^{15}N abundance of soil nitrate (total number of ^{15}N-labelled nitrate molecules in the studied soil). This is especially relevant for long incubations (>10 h in the cases of Cuhel et al., 2010; Morse and Bernhardt 2013; Sgouridis and Ullah, 2015 or Xi et al., 2022); although ideally, incubations should be kept to a minimum time (< 3 hours, Friedl et al., 2020).

It would be very difficult to assess generalities, as the magnitude of transformation of nitrates will vary greatly from one soil to another. Experimental data show that the disappearance of the label can be quite slow. Stevens et al. (1997) observed a decrease from 10% to 5% over ten days and under three different moisture contents (Fig. 3 d,e,f, of cited reference). Ruser et al. (2006) observed very little variations over 70 days, usually less than 10% drop (Fig. 4 of cited reference). Bergsma et al. (1999) observed a drop from 82% to 72% after three days and half. Rummel et al. (2021) observed different patterns of dilution of the ^{15}N label for different fertilization/plant treatments over a 10-day period (Fig. 3 of the cited reference). Although quite variable, we can observe that only a small decrease occurs within the first days.

If a significant drop in the ^{15}N abundance is observed however, it is possible to use the heuristic model of Bergsma et al. (1999) to have an estimation of the induced error and correct for the dilution effect.

3.2. Formation of hybrid N_2 and N_2O

The full extent of microbial metabolic transformations in soil is still not totally understood today, yet several reactions could affect the calculations of the ^{15}NGF through formation of hybrid N_2 and N_2O molecules. The term "hybrid" here refers to the fact that within the same molecule, one nitrogen atom comes from the labelled nitrate pool while the other one comes from another source (considered at natural ^{15}N abundance if not labelled). Reactions leading to the formation of hybrid N_2 and N_2O include co-denitrification, anammox and other abiotic processes (Phillips et al., 2016). Co-denitrification was formally identified in the laboratory by Shoun et al. (1992) when amending a fungal strain ("*Fusarium oxysporum*") with NO_3^- enriched at 99% in ^{15}N atoms and observing a significant signal at m/z = 29 through a mass spectrometer. This meant that a large number of $^{29}N_2$ molecules were denitrified, which was not possible given that the nitrate pool was almost exclusively labelled with ^{15}N atoms, which should have led to the production of $^{30}N_2$ molecules only. Tanimoto et al. (1992) demonstrated that one of the two nitrogen atoms was derived from the organic pool of the soil (azide compounds and salicylhydroxamic acid in the case of their study). As explained by Spott et al. (2011b), co-denitrification is microbially mediated around neutral pH and most co-denitrifying species are already known as regular denitrifiers (*Pseudomonas* sp., *Fusarium* sp., etc.). Furthermore, co-denitrification has already been reported to occur within the three domains Archaea, Bacteria, and Eukarya. Little is known about this process, including its potential magnitude during *in situ* measurements and unfortunately, relatively few studies have focused on its measurement (Laughlin and Stevens, 2002; Spott and Florian Stange, 2011a; Long et al., 2013; Selbie et al., 2015; Lewicka-a-Szczebak et al., 2017; Clough et al., 2017; Rohe et al., 2021). In particular, Laughlin and Stevens (2002) found that 92% of the emitted N_2 was due to co-denitrification rather than denitrification in their study, while Selbie et al. (2015) found a similar percentage of 97%. Lewicka-Szczebak et al. (2017) detected lower contribution from co-denitrification (18% and 5% respectively in two different experiments).

Anammox is the biological process that converts NO_3^- and NH_4^+ into N_2. It is of primary importance in coastal, aquatic and oceanic ecosystems (Thamdrup and Dalsgaard, 2002). However, anammox bacteria have been found in different terrestrial ecosystems such as marshes, lakeshores, permafrost soils or agricultural soils (Humbert et al., 2010).

Abiotic processes leading to the formation of hybrid N_2 and N_2O molecules include chemo-denitrification and decomposition of hydroxylamine (see Phillips et al., 2016 and Zhu-Barker et al., 2015 for further explanations of these processes).

Phillips et al. (2016) described precisely the different ways hybrid N_2 or N_2O molecules can be formed but overall, biotic co-denitrification is probably the predominant process in terrestrial systems.

3.2.1. Simulation: how could the presence of hybrid N_2 and N_2O molecules affect the calculations of the ^{15}NGF?

It could be hypothesized that subsequent to the previously mentioned work of Boast et al. (1988), the ^{15}N abundance of the soil denitrifying pool $\boldsymbol{a_p}$ should be overestimated and the proportion of N_2 molecules deriving from denitrification $\boldsymbol{d}$ underestimated since there is a second pool of nitrogen in the soil. The case is very different here because of the hybrid molecules. The labelled nitrate pool is still considered at isotopic equilibrium, but the hybrid molecules have a different isotopologue distribution. For the emitted N_2 molecules, this distribution can be expressed as:

$$\%^{28}N_2 = (1-\mathrm{H})\left(1-a_p\right)^2 + H\left(1-a_p\right)\left(1-a_a\right) \quad [7a]$$

$$\%^{29}N_2 = (1-H)2a_p\left(1-a_p\right) + H\left(a_a\left(1-a_p\right) + a_p\left(1-a_a\right)\right) \quad [7b]$$

$$\%^{30}N_2 = (1-H)a_p^2 + H\left(a_p a_a\right) \quad [7c]$$

Note the appearance of a new term $\boldsymbol{H}$. It refers to the fraction of emitted hybrid N_2 (hence $0 < \boldsymbol{H} < 1$) and includes all sources of hybrid molecules. We consider the pool of co-substrate (from which the second N atom derives in the hybrid N_2 and N_2O molecules) at natural ^{15}N abundance $\boldsymbol{a_a}$ and we note again $\boldsymbol{a_p}$ the ^{15}N abundance of the soil denitrifying pool. Note that the distribution of isotopologues is analogous to that of Spott and Stange (2011a, equations 1, 2 and 3), although here there is no contribution of purely non-hybrid denitrification from the co-substrate. In their case, the organic co-substrate (hydroxylamine) could be denitrified on its own abiotically but we will take the more general case where the pool of co-substrate cannot perform denitrification on its own.

Let us compare the ratios R29 and R30 after incubation in the case of pure denitrification and in the case where some hybrid molecules are emitted ($\boldsymbol{H} \neq 0$) for the same amount of total denitrified molecules (same coefficient $\boldsymbol{d}$):

$$R29_D = \frac{(1-d)[2a_a(1-a_a)] + d\left[2a_p\left(1-a_p\right)\right]}{(1-d)(1-a_a)^2 + \mathrm{d}\left(1-a_p\right)^2} \quad [7d]$$

The subscript "D" refers to the case of classic denitrification and "H" to the case where hybrid sources are present.

With the presence of hybrid molecules, the coefficient $\boldsymbol{d}$ is renamed "$\boldsymbol{d_{total}}$" and can be more explicitly defined as:

$$d_{total} = d_{denitrification} + d_{hybrid} \quad [7h]$$

where,

$$d_{denitrification} = (1-H) \times d_{total} \quad [7i]$$

$$d_{hybrid} = H \times d_{total} \quad [7j]$$

Similarly, we define:

$$a_{p\ total} = H\left(\frac{a_a + a_p}{2}\right) + (1-H)a_p \quad [7k]$$

Which is the ^{15}N enrichment of the emitted molecules and could be considered as the apparent ^{15}N enrichment of the soil denitrifying pool, which includes the non-labelled pools contributing to the formation of hybrid molecules.

Given the complexity of the calculations, we made a simulation using Excel (Microsoft, Redmond, WA). For six realistic values of $\boldsymbol{a_p}$ (5%, 10%, 20%, 30%, 40% and 50%), eleven realistic values of $\boldsymbol{d}$ (ranging from 1.10^{-8} to 1.10^{-3}) were used with nine values of H (from 0.01% to 100%) as shown in Table S1 from the **Annex 1** (**Supporting Information**), to create 594 different cases. Using a perfect distribution of isotopologues (as per equations [7d] to [7g]), the ideal gas law and assuming atmospheric pressure inside a chamber of 4 L, ideal values of R29 and R30 have been calculated. Then, using the calculations of both Arah (1992) and Mulvaney and Boast (1986), the ^{15}N abundance of the soil denitrifying pool $\boldsymbol{a_{p\ calculated}}$ and the coefficient $\boldsymbol{d_{calculated}}$ have been back-calculated as they would be if ignoring the contribution of co-denitrification. These values have been compared to their real counterpart values used for the simulations and error has been determined as a percentage as:

$$\%err\ d_{total} = 100\left(\frac{d_{calculated} - d_{total}}{d_{total}}\right) \quad [8a]$$

$$\%err\ d_{denitrification} = 100\left(\frac{d_{calculated} - d_{denitrification}}{d_{denitrification}}\right) \quad [8b]$$

The first equation refers to the error made in the quantification of all emitted molecules ($\boldsymbol{d_{total}}$) where the second equation refers to the error made regarding only the purely non-hybrid molecules emitted through classic denitrification ($\boldsymbol{d_{denitrification}}$).

Similarly, we define:

$$R29_H = \frac{(1-d)[2a_a(1-a_a)] + d\left[(1-H)2a_p\left(1-a_p\right) + H\left(a_a\left(1-a_p\right) + a_p\left(1-a_a\right)\right)\right]}{(1-d)(1-a_a)^2 + \mathrm{d}\left[(1-\mathrm{H})\left(1-a_p\right)^2 + H\left(1-a_p\right)\left(1-a_a\right)\right]} \quad [7e]$$

$$R30_D = \frac{(1-d)a_a^2 + d\left(a_p\right)^2}{(1-d)(1-a_a)^2 + \mathrm{d}\left(1-a_p\right)^2} \quad [7f]$$

$$R30_H = \frac{(1-d)a_a^2 + d\left[(1-H)a_p^2 + Ha_p a_a\right]}{(1-d)(1-a_a)^2 + \mathrm{d}\left[(1-\mathrm{H})\left(1-a_p\right)^2 + H\left(1-a_p\right)\left(1-a_a\right)\right]} \quad [7g]$$

$$\%err\ a_{p\ total} = 100\left(\frac{a_{p\ calculated} - a_{p\ total}}{a_{p\ total}}\right) \quad [8c]$$

$$\%err\ a_{p\ denitrification} = 100\left(\frac{a_{p\ calculated} - a_{p\ denitrification}}{a_{p\ denitrification}}\right) \quad [8d]$$

which refer to the errors made in the calculation of the ^{15}N-enrichment of the soil denitrifying pool considering respectively, the total apparent enrichment ($\boldsymbol{a_{p\ total}}$) or the enrichment of the labelled pool only ($\boldsymbol{a_{p\ denitrification}}$).

3.2.2. Results of the simulation

Firstly, it should be noted that the values obtained in the cases where $H = 100\%$ will not be taken in account as the coefficients $d_{calculated}$ are superior to 1. It seems that the ^{15}NGF does not work when H becomes very close to 100%. It still gives a coefficient d inferior to 1 for $H = 99.90\%$ (at which point the error on $d_{total} > 1\,000\%$ however) but not if $H = 99.99\%$. Similarly, we will not study the cases where $H = 0.01\%$ and $H = 0.1\%$ because the repartition of errors at these levels is somewhat more chaotic than in the other cases. However, the magnitude of error on d_{total}, $d_{dentrification}$, $a_{p\ total}$ and $a_{p\ denitrification}$ for $H = 0.01\%$ and $H = 0.1\%$ is more than negligible as can be seen in Table S2 (**Annex 1**, **Supporting Information**). Also, the estimations of d_{total}, $d_{dentrification}$, $a_{p\ total}$ and $a_{p\ denitrification}$ based on either the method of Arah (1992) or Mulvaney and Boast (1986) did not differ significantly. Although the calculations of Mulvaney and Boast (1986) were more accurate in 263 cases out of 396 (we did not consider the cases where $H = 100$, 0.1 or 0.01%), the difference between the two methods was always less than 0.2%.

The first objective was to determine the correlations between the three parameters (H, d and a_p) and the errors made on d_{total}, $d_{dentrification}$, $a_{p\ total}$ and $a_{p\ denitrification}$.

Thus, correlation tests were run with SPSS (IBM Corp. Released, 2019. IBM SPSS Statistics for Windows, Version 26.0. Armonk, NY: IBM Corp) using either Kendall's tau-b or Spearman coefficients. We did not use the Pearson coefficient as upon visual inspection and Shapiro-Wilk tests, the errors were never distributed normally. The correlation tests were run on sub-datasets where two parameters were constant while the studied one varied. The results in Table S3 (**Annex 1**, **Supporting Information**) show that the errors made on d_{total}, $d_{dentrification}$, $a_{p\ total}$ and $a_{p\ denitrification}$ are all independent of d and dependent of H. On the other hand, the errors on $a_{p\ total}$ and $a_{p\ denitrification}$ were dependent on a_p where the ones on d_{total} and $d_{dentrification}$ were not.

Obviously, the ^{15}N abundance of the soil denitrifying pool ($a_{p\ denitrification}$) will be underestimated due to the presence of unlabelled pools contributing to the formation of hybrid molecules. The results of this simulation indicate that the apparent ^{15}N abundance of the denitrifying pool ($a_{p\ total}$) will also be underestimated when hybrid molecules are formed. This can be seen in Figs. S1 and S2 (**Annex 1**, **Supporting Information**) which show the evolution of the errors made on $a_{p\ total}$ and $a_{p\ denitrification}$ with either H or a_p for different scenarios. All of these errors are negative, thus causing a systematic underestimation. This is contrary to the conclusions of Boast et al. (1988) who showed that the ^{15}N abundance of the soil denitrifying pool should be overestimated when multiple pools are present. However, the case here is different again because the presence of hybrid molecules changes the distribution of isotopologues. Similarly, the presence of hybrid sources systematically causes an overestimation of the fraction d (either d_{total} or $d_{denitrification}$), inversely to the case of multiple pools in isotopic equilibrium as described by Boast et al. (1988). We can see this result in Table S4 (**Annex 1**, **Supporting Information**) which shows the average errors made on d_{total} and $d_{dentrification}$ for different values of H. These averages were calculated using all combinations of a_p and d for the same values of H (n = 66), since it was shown that the errors on d_{total} and $d_{dentrification}$ were not correlated with a_p and d. Using this property, we can extrapolate the results of a specific case (fixed a_p and d) to represent the evolution of the errors made on d_{total} and $d_{dentrification}$ with H for all cases. Fig. 4 represents this evolution for the case $a_p = 40\%$ and $d = 1.10^{-4}$ that we will consider a general trend here. This means that no matter how enriched the soil denitrifying pool is or the amount of soil-emitted molecules, the error caused by the presence of hybrid molecules can be read on Fig. 4.

It can be seen from Fig. 4 that, no matter the quantity of tracer used or the number of emitted molecules, the overestimation of the total number of molecules is insignificant (<1%) until the contribution of hybrid molecules reaches approximately 20%. At 50% of hybrid contribution, the overestimation is 12.5% which can still be acceptable given the general accuracy of the ^{15}NGF. Higher hybrid source contributions however cause great overestimation (80% for $H = 80\%$) until H becomes very close to 100%, at which point the error tends to infinity. If studying the quantity of molecules solely emitted through classic denitrification, then the overestimation increases drastically. It reaches 1% when $H = 1\%$ already, 26% when $H = 20\%$ and predicts more than twice the real amount when $H = 50\%$.

We verified that all these results and trends were still valid even at a very high enrichment of the soil denitrifying pool and found similar results even at the extreme limit $a_p = 100\%$.

Since the errors made on d_{total}, $d_{dentrification}$, $a_{p\ total}$ and $a_{p\ denitrification}$ are not correlated with the parameter d, the same conclusions should be drawn for N_2O. The study is similar with the exception of the atmospheric background being much smaller (around 0.330 ppm_v) and thus higher d values are typically found. We tested this hypothesis by duplicating the N_2 tables and by only changing the atmospheric background and the range of d values used in the simulations (see Table S1 in **Annex 1**, **Supporting Information**). Thus, for sub-datasets of constant H and a_p values, we compared the means of the errors made on d_{total}, $d_{dentrification}$, $a_{p\ total}$ and $a_{p\ denitrification}$ for N_2 and N_2O and expressed a relative difference as:

$$\%err\ W(N_2 - N_2O) = 100\left|\frac{W_{N_2O} - W_{N_2}}{W_{N_2}}\right| \quad [8e]$$

where W is the mean of the errors made on either d_{total}, $d_{dentrification}$, $a_{p\ total}$ or $a_{p\ denitrification}$ for sub-datasets of constant H and a_p values (n = 11). Table S5 (**Annex 1**, **Supporting Information**) shows that on average, the model for N_2O did not vary significantly from the model for N_2. The highest relative mean of error difference between the two models was for d_{total} and was 1.5×10^{-3} %, the highest coefficient of variation (CV) of a sub-dataset of constant H and a_p values was 1.18×10^{-8} %; thus, we will consider that similar conclusions can be drawn for N_2 and N_2O.

In conclusion, the formation of hybrid molecules affects N_2 and N_2O emissions similarly (given that the same organism reduces NO and N_2O to N_2O and N_2, respectively). In contrast to the heterogeneous application of the tracer (assumption 1, part 3.1 of this study), it causes an overestimation of the measured quantity of molecules (both the total amount of evolved molecules and the purely denitrified ones) and an underestimation of the enrichment of the soil denitrifying pool (both the total apparent pool which includes the co-substrates and the labelled nitrate pool). The overestimation of the flux does not depend on the quantity of tracer injected (^{15}N enrichment of the soil denitrifying pool a_p) nor the total quantity of emitted molecules (d) but only on the proportion of hybrid molecules (parameter H). This might not be true at very low contribution of hybrid molecules (H<1%) but the magnitude of error at this level is so low that it does not really matter. We can add that the underestimation of the ^{15}N enrichment depends on the quantity of tracer injected and the proportion of hybrid molecules, but not on the number of emitted molecules. The total apparent enrichment ($a_{p\ total}$) is not a crucial parameter since the hybrid pool is not at isotopic equilibrium and thus the isotopologue distribution from this source cannot be determined with it. But it could be an important tool, especially if one wants to prove that hybrid sources contribute to denitrification.

These results are in accordance with the study of Spott and Stange (2007), which found that denitrification is indeed overestimated when hybrid molecules are formed. Their study only focused on the overestimation of purely denitrified molecules ($d_{denitrification}$, which is called "B" in the cited study, see Fig. 3 of Spott and Stange, 2007). However, we did not find that this overestimation was dependent on the ^{15}N enrichment of the soil nitrate pool, nor on the fraction of atmospheric N_2 (neither with the model of Arah nor with the model of Mulvaney & Boast). We did find however, as in the study of Spott and Stange (2007), that this overestimation is dependent on the proportion of emitted hybrid molecules.

3.2.3. Mitigation

Laughlin and Stevens (2002) have developed a method to calculate the contribution of co-denitrification based on previous work by Clough et al. (2001). This model should be applicable no matter the process (or processes) emitting hybrid molecules in a mix with classic denitrification and atmosphere. However, it is important to remember that this method is largely dependent on the assumption that the soil denitrifying pool is at isotopic equilibrium, which as shown before, is unlikely to be true due to heterogeneous distribution of the ^{15}N label (see part 3.1 of this study). Violation of this principle could even lead to the assumption that hybrid molecules are being emitted when actually, only classic denitrification is occurring. The best solution would be to confirm the presence of hybrid molecules before trying to calculate their contribution, which is unfortunately not easy. Clough et al. (2001) demonstrated that $\frac{\Delta R29}{\Delta R30} = 272$ when co-denitrification occurs (or other processes emitting hybrid molecules) but it is very important to note that this is only the case when all emitted molecules are hybrid ($\boldsymbol{H} = 100\%$). In the case of classic denitrification ($\boldsymbol{H} = 0$), the quantity $\frac{\Delta R29}{\Delta R30}$ only depends on the ^{15}N enrichment of the soil denitrifying pool (the natural ^{15}N abundance of the atmosphere being considered constant). This can be seen in equation 17 of the study of Mulvaney and Boast (1986). Thus, if the quantity $\frac{\Delta R29}{\Delta R30}$ is not equal to its hypothetic value using the ^{15}N abundance of the soil denitrifying pool, one might suspect the presence of hybrid molecules as in Laughlin and Stevens (2002). However again, because the soil isotopic equilibrium hypothesis might be violated, this might not be a reliable option. Spott and Stange (2007) have developed a model to quantify the contributions of anammox and denitrification to N_2 emissions in aquatic environments when both processes are occurring simultaneously, based on previous work from Thamdrup and Dalsgaard (2002). According to Spott and Stange (2007), this model can also be used for terrestrial systems when hybrid molecules are emitted. The case is more delicate here however, since the atmosphere plays a much bigger part in the mix, reducing greatly the sensitivity. The authors also emphasized the need to know if hybrid molecule sources are actually present before using this model. Spott and Stange (2011a) proved the presence of a source of hybrid molecules in soil using a sophisticated system combining a soil suspension in water and a flushing of the headspace by a stream of Helium. Precise equations for the exact determination of the contributions of non-hybrid and hybrid molecules were derived as well as the factor R_{binom}, which enables quick assessment of the presence of multiple sub-pools (see part 3.1.1 of this study) or hybrid molecules. Unfortunately, this precise model can only be used in the absence of atmospheric N_2 (using a Helium atmosphere in the example of the cited study), which complicates its use. These new equations were later used by Lewicka-Szczebak et al. (2017) under artificial atmosphere which might explain why they found a more reasonable percentage of co-denitrification (5 and 18% in two different experiments) than Laughlin and Stevens (2002) or Selbie et al. (2015), who both used the method of Laughlin and Stevens (2002) and found contributions of 92 and 97% respectively of co-denitrification. Fig. 4 shows that if these two contributions were true, applying the ^{15}NGF without taking them in account would result in high overestimations (>260 and 780% respectively for $\boldsymbol{d_{total}}$, and >4 400 and 29 000% respectively for $\boldsymbol{d_{denitrification}}$). The contributions of 5 and 18% found by Lewicka-Szczebak et al. (2017) would result in overestimations of 0.07 and 0.99% respectively for $\boldsymbol{d_{total}}$, and 5.33 and 23.16% respectively for $\boldsymbol{d_{denitrification}}$.

3.3. Quantitative recovery of denitrification products in the flux chamber

Similarly to other incubation techniques, the ^{15}NGF is subject to error due to diffusive losses when used *in situ*. As Myrold (1990) mentioned, the fluxes of gas emissions from soil are a function of not only the production rate but also transport processes. Although convective movements can occur, diffusion is considered the predominant process of gas transport in soil (Clough et al., 2005). Diffusion in one dimension can be modelled by Fick's first law, which states that the diffusion of molecules is proportional to the gradient of their concentration:

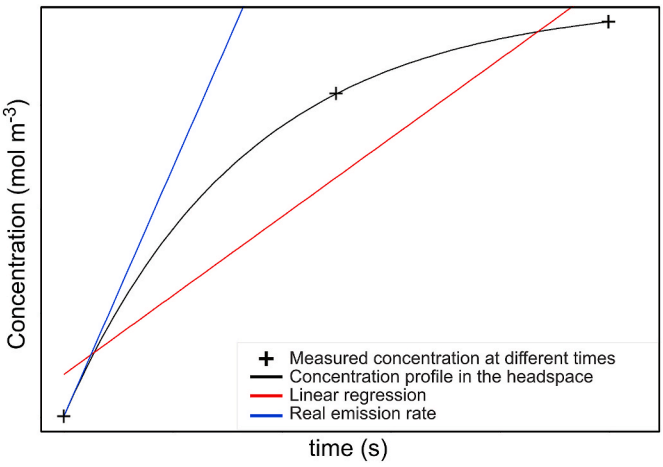

Fig. 5. Theoretical evolution of unlabelled N_2O concentration inside an accumulation chamber with time (black). The red line represents a linear regression made using the three hypothetic measurements made at different times (black crosses). The blue line represents the real emission rate of N_2O, as would be measured without the diffusion issues caused by the accumulation of emitted N_2O inside the headspace of the chamber.

$$J_i = -D_i \frac{dC_i}{dz} \quad [9a]$$

Where $\boldsymbol{J_i}$ is the flux of molecules of the species $\boldsymbol{i}$ (in mol m^{-2} s^{-1}), $\boldsymbol{C_i}$ is the concentration of the species $\boldsymbol{i}$ (in mol m^{-3}), $\boldsymbol{D_i}$ is the binary gas coefficient of the species $\boldsymbol{i}$ (in m^2 s^{-1}), and $\boldsymbol{z}$ is the distance from the production zone in this case.

In a first approximation for short-term experiments and for unlabelled gases (N_2O in this case), Hutchinson and Mosier (1981) suggested the following model to predict the evolution of concentration of unlabelled N_2O inside a chamber based on Fick's first law:

$$\frac{dC_t}{dt} = \frac{A}{V}\frac{D_p}{d}(\varphi - C_t) \quad [9b]$$

Equation [9b] was rewritten with the nomenclature of Pedersen (2000), where $\boldsymbol{\varphi}$ is the hypothetical constant concentration (mol m^{-3}) in the production zone at the depth $\boldsymbol{d}$ (m), $\boldsymbol{C_t}$ is the headspace concentration (mol.m^{-3}) at time $\boldsymbol{t}$, $\boldsymbol{V}$ is the volume of the headspace in the chamber (m^3), $\boldsymbol{A}$ is the area of soil incubated (m^2) and $\boldsymbol{D_p}$ is the binary molecular diffusion coefficient of the studied gas in the air at ambient temperature and pressure (in $m^2.s^{-1}$).

It is possible to theoretically resolve the model of Hutchinson and Mosier (1981) to determine the concentration profile of unlabelled N_2O in the headspace of the chamber as a function of time (Pedersen et al., 2010):

$$C(t) = \varphi + (C_0 - \varphi)e^{(-\kappa t)} \quad [9c]$$

With $\kappa = \frac{D_p \times A}{V \times d}$.

Plotting this evolution as in Pedersen et al. (2001) gives a good idea of how underestimation of a non-labelled gas flux can happen, as illustrated in Fig. 5.

The concentration initially increases in an almost linear trend but as accumulation occurs in the headspace of the chamber, this trend slowly declines to reach a plateau. Measuring the initial flux $f_0 = \frac{V}{A}\frac{dC}{dt}_{t=0}$ is thus the best estimate of the magnitude of gas emissions since the effects of diffusion are negligible at that time. If diffusion is ignored and a linear model is applied, then the emission rate is largely underestimated (slope

Table 3
Main diffusion models applicable for measurement of a non-labelled greenhouse gas using an accumulation chamber.

Method	Profile	Pros	Cons	Reference
Linear regression	Line	Easy and does not require more than two measurements per plot.	Probably the least accurate estimation.	Forthofer et al. (2007).
Hutchinson and Mosier (1981) ("HM")	Exponential	Needs "only" three measurements per plot, improved accuracy.	Relies on the condition $\frac{(C_1 - C_0)}{(C_2 - C_1)} > 1$ (where C_n is the concentration at the time step **n**), which is not true always true. Needs regular time intervals between measurements.	Hutchinson and Mosier (1981), Anthony et al. (1995).
Stochastic model	Exponential	HM approach but more than 3 points can be used for better sensitivity, time intervals don't have to be equals.	Complicated mathematical expression.	Pedersen et al. (2010), , Pedersen et al. (2001).
Quadratic model	Quadratic	Easier than other models.	Does not take in account the complex physical and physiological mechanisms of gas emission in soil.	Wagner et al. (1997).
Non-steady-state Diffusive Flux Estimator (NDFE)	Square root (at long times)	Uses the general equation of diffusion (more precise).	Complicated mathematical expression.	Livingston et al. (2006), Hossler and Bouchard (2008).
Extended HM	Exponential	Robust against horizontal gas transport and patterns of non-linearity. Included in the "HMR" R package available on CRAN (http://www.r-project.org).	Qualified handling of data in the concentration range near the detection limit of the experimental system.	Pedersen et al. (2010).

Parkin et al. (2012) reviewed most of these models for comparison (at the exception of the stochastic extension of the HM and the NDFE models) and estimated their limits of detection.

of the red line compared to the slope of the blue line). Several models of diffusion have been developed for non-labelled gases and are summed up in Table 3.

The case is however different with the ^{15}NGF due to the presence of ^{15}N-labelled molecules. Firstly, we can note that the one-dimensional law of Fick mentioned above is normally defined for a binary mix and is somewhat simplistic. The real multicomponent model is described by the equations of Stefan and Maxwell, which are more complex. Jaynes and Rogowski (1983) showed, however, that for a tracer in a multicomponent mix, the tracer will diffuse according to Fick's first law. A new diffusion coefficient $\boldsymbol{D_{Fi}}$ must be calculated as shown by equation 17 of the cited reference. Furthermore, in soil, the flux J_i needs to be multiplied by a coefficient of tortuosity $\boldsymbol{\tau}$ and the air-filled porosity of the soil $\boldsymbol{\varepsilon}$ (m^3 of air per m^3 of soil) to better describe the heterogeneous nature of this medium (Jaynes and Rogowski, 1983; Hutchinson and Livingston, 2002). This leads to the following relation:

$$J_i = -\tau\varepsilon D_{Fi}\frac{dC_i}{dz} \quad [9d]$$

The complexity of the system leads to the calculation of new (and somewhat challenging) parameters but overall, the diffusion of ^{15}N-labelled molecules is still ruled by a Fickian model. This means that these new parameters can be determined with experimental data.

The main issue with the gas dynamics in the ^{15}NGF however, is that the production of ^{15}N-labelled gases (N_2 and N_2O alike) after labelling causes build-up of their concentration in pore space (referred as "storage flux"). This leads to fluxes according to concentration gradients (Fick's first law) to the atmosphere, but also to the subsoil, sooner or later reaching a steady state concentration profile in case of a constant production. Already at this steady state, before closing the flux chamber, a significant part of the produced gases diffuses to subsoil (up to 40% according to Well et al., 2019b). Closing the chamber leads to increasing concentration of ^{15}N-labelled molecules inside the chamber headspace, leading to a decrease in surface flux with accumulation time while subsoil and storage fluxes go up.

The total flux of denitrification is the sum of the surface, storage and subsoil fluxes; but only the surface flux is measured with the ^{15}NGF. Therefore, diffusion dynamics lead to severe underestimation of denitrification if subsoil and storage fluxes are not taken into account, where this bias is higher for extend accumulation times. Well et al. (2019b) showed that the ratio between surface flux to the sum of storage and subsoil fluxes at a given accumulation time depends on the geometry of the cylinder confining the ^{15}N-labelled soil, the depth distribution of the ^{15}N label, depth of distribution of denitrification, gas diffusivity and soil moisture. The share of surface flux increases with soil moisture, diffusivity and length of confinement (height of the collar confining the labelled soil). It decreases with depth of labelling and accumulation time.

Well et al. (2019b) showed through simulation that ignoring diffusive losses could lead to great underestimation (from 28% to 71%) but a parallel field study using a bottom-closed cylinder showed that their model was not in perfect adequacy with the experiment, predicting twice the observed underestimation. This is largely due to the inability to assess the complexity of the processes occurring in the soil, especially temporal and spatial dynamics of denitrification as well as diffusivity. Nonetheless, the bottom-closed cylinder experiment revealed an underestimation of 37% of the flux of denitrification due to diffusive losses.

It can also be said that increased storage flux can modify the product ratio of denitrification (equation [6b]). Indeed, accumulation of N_2O in pore space tends to favour N_2O reduction into N_2 (Well et al., 2019b).

There is no evident solution to mitigate the effects of diffusion on the ^{15}N-labelled molecules for accurate measurement of denitrification with the ^{15}NGF. Using a diffusion model as presented in Table 3 will only get a more accurate estimation of the surface flux at $t = 0$ and will not account for subsoil and storage fluxes. While a bottom closed cylinder as in Well et al. (2019b) is principally suitable, it leads to serious disturbance of the soil and root system and is thus not adequate for continuous experiments with repeated sampling. The main strength of the ^{15}NGF is precisely the possibility to be used *in situ* with little disturbance to the soil. The other solution could be to a use simulation as in Well et al. (2019b) and allow sufficient time after labelling the soil (few hours to a day; since it was shown in part 3.1.2 of this study that soil is still labelled for at least several days after application of the tracer) before closing the flux chamber. This would allow equilibration of the tracer solution and build-up of near-steady-state profiles of gas concentrations and diffusive fluxes. Finally, enclosure time should be kept to a minimum (< 3 hours, Friedl et al., 2020).

Table 4
Simulation of the sensitivity of the ^{15}NGF.

a_p	d	Flux (gN/ha/d)	ΔR29	ΔR30
5%	1E-08	0.19	8.90E-10	2.51E-11
	5E-08	0.94	4.45E-09	1.25E-10
	1E-07	1.88	8.90E-09	2.51E-10
	5E-07	9.36	4.45E-08	1.25E-09
	1E-06	18.74	8.90E-08	2.51E-09
	5E-06	93.6	4.45E-07	1.25E-08
	1E-05	187.4	8.90E-07	2.51E-08
	5E-05	936	4.45E-06	1.25E-07
	1E-04	1874	8.90E-06	2.51E-07
	5E-04	9366	4.45E-05	1.25E-06
10%	1E-08	0.19	1.75E-09	1.01E-10
	5E-08	0.94	8.77E-09	5.03E-10
	1E-07	1.88	1.75E-08	1.01E-09
	5E-07	9.36	8.77E-08	5.03E-09
	1E-06	18.74	1.75E-07	1.01E-08
	5E-06	93.6	8.77E-07	5.03E-08
	1E-05	187.4	1.75E-06	1.01E-07
	5E-05	936	8.77E-06	5.03E-07
	1E-04	1874	1.75E-05	1.01E-06
	5E-04	9366	8.76E-05	5.03E-06
20%	1E-08	0.19	3.18E-09	4.03E-10
	5E-08	0.94	1.59E-08	2.01E-09
	1E-07	1.88	3.18E-08	4.03E-09
	5E-07	9.36	1.59E-07	2.01E-08
	1E-06	18.74	3.18E-07	4.03E-08
	5E-06	93.6	1.59E-06	2.01E-07
	1E-05	187.4	3.18E-06	4.03E-07
	5E-05	936	1.59E-05	2.01E-06
	1E-04	1874	3.18E-05	4.03E-06
	5E-04	9366	1.59E-04	2.01E-05
30%	1E-08	0.19	4.19E-09	9.07E-10
	5E-08	0.94	2.10E-08	4.53E-09
	1E-07	1.88	4.19E-08	9.07E-09
	5E-07	9.36	2.10E-07	4.53E-08
	1E-06	18.74	4.19E-07	9.07E-08
	5E-06	93.6	2.10E-06	4.53E-07
	1E-05	187.4	4.19E-06	9.07E-07
	5E-05	936	2.10E-05	4.53E-06
	1E-04	1874	4.19E-05	9.07E-06
	5E-04	9366	2.10E-04	4.53E-05
40%	1E-08	0.19	4.81E-09	1.61E-09
	5E-08	0.94	2.40E-08	8.06E-09
	1E-07	1.88	4.81E-08	1.61E-08
	5E-07	9.36	2.40E-07	8.06E-08
	1E-06	18.74	4.81E-07	1.61E-07
	5E-06	93.6	2.40E-06	8.06E-07
	1E-05	187.4	4.81E-06	1.61E-06
	5E-05	936	2.40E-05	8.06E-06
	1E-04	1874	4.81E-05	1.61E-05
	5E-04	9366	2.40E-04	8.06E-05
50%	1E-08	0.19	5.02E-09	2.52E-09
	5E-08	0.94	2.51E-08	1.26E-08
	1E-07	1.88	5.02E-08	2.52E-08
	5E-07	9.36	2.51E-07	1.26E-07
	1E-06	18.74	5.02E-07	2.52E-07
	5E-06	93.6	2.51E-06	1.26E-06
	1E-05	187.4	5.02E-06	2.52E-06
	5E-05	936	2.51E-05	1.26E-05
	1E-04	1874	5.02E-05	2.52E-05
	5E-04	9366	2.51E-04	1.26E-04

Simulation of the sensitivity of the ^{15}NGF through a 1-h incubation using a 4L chamber (0.05 m^2 basal area) with different values of a_p and d, considering isotopic equilibrium of atmospheric and soil denitrifying pools, atmospheric pressure and the ideal gas law. Values in red cannot be detected with routinely available IRMS where values in yellow could be with higher sensitivity instruments. Values in green can be detected.
Colour code: ΔR29: Red $< 9.1 \times 10^{-7} <$ Yellow $< 8.0 \times 10^{-6} <$ Green
ΔR30: Red $< 3.2 \times 10^{-7} <$ Yellow $< 9.8 \times 10^{-7} <$ Green

3.4. Stimulation of denitrifying microbes (fertilization effect)

As the ^{15}N tracer is injected in the form of a nitrate solution (the substrate of denitrification), it is possible that microbial activity may be stimulated and thus more denitrification products emitted, leading to an overestimation of this process. Although acknowledged by various authors (Groffman et al., 2006; Sgouridis and Ullah, 2015; Dodds et al., 2017; Warner et al., 2019; Lewicka-Szczebak and Well, 2020a) it has not in fact been investigated extensively. As mentioned by Groffman et al. (2006), Yang et al. (2014) and Sgouridis and Ullah (2015), this is mainly an issue in natural environments where low levels of nitrogen are available, typically where the only sources of nitrogen are natural (such as fixation and mineralization) or eventually from atmospheric deposition. On the other hand, agricultural lands managed under intensive nitrogen fertilization should not be as sensitive to added nitrates.

When studying denitrification in agricultural soil, Loick et al. (2017) "fed" microbes large amounts of nitrate and glucose. This resulted in higher N_2O and N_2 emissions compared to their control treatment (see Fig. 2 of the cited reference). Similarly, Clayton et al. (1997) studied the influence of different nitrogen treatments on denitrification from fertilised grasslands over two years. In Fig. 1 of the cited reference, it is visible that when treated with calcium nitrate (CN), N_2O fluxes are considerably greater than the control. It is also worth mentioning that the added nitrates particularly stimulated emissions under wet and warm conditions in the same study (by almost two orders of magnitude). Jarvis et al. (1991) also correlated high *in situ* rates of denitrification with fertilizer application, especially again when the soils were wet or after a rainfall event.

It is difficult to compare these studies to the use of the ^{15}NGF given that the amount of applied tracer will vary from one study to another (and will be much lower than a fertilizer application); but they show however that a denitrification stimulation can occur when adding nitrate to soil. Ideally, further studies would be necessary to thoroughly assess the impact of added nitrates on the denitrification process under the use of the ^{15}NGF, but some fertilization effect has to be accepted (especially for the natural environment), and thus observed rates may have to be interpreted with care. In agricultural systems, the tracer is often injected to mimic a realistic fertilization input from farming practices as in Buchen et al. (2016). In such a case, we can expect a stimulation as observed in the studies mentioned in the previous

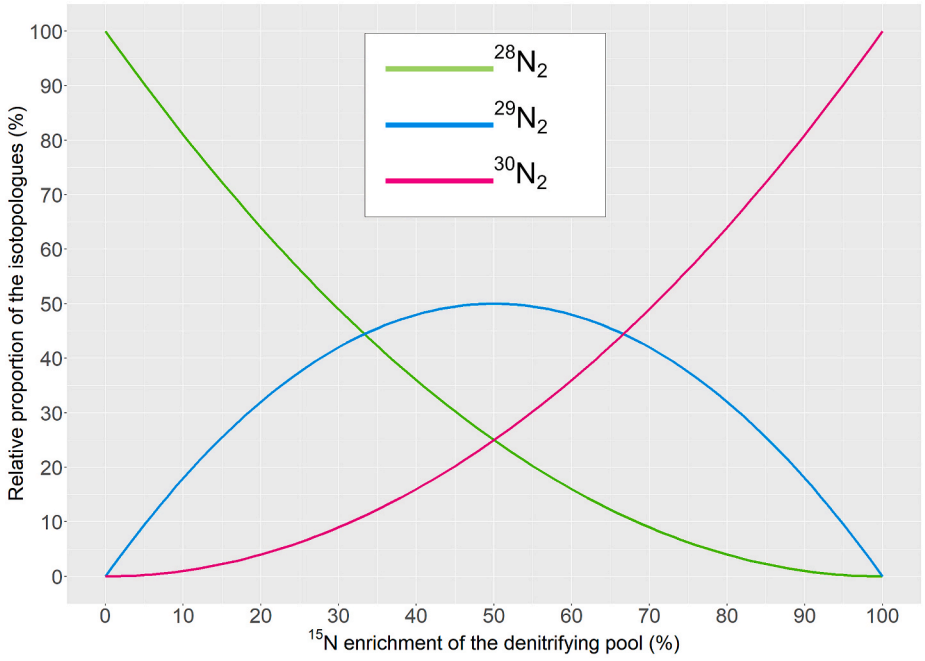

Fig. 6. Evolution of the three N_2 isotopologue proportions for different values of the soil denitrifying pool ^{15}N abundance (considering isotopic equilibrium). The proportion of $^{29}N_2$ is maximal for a ^{15}N enrichment of 50%.

paragraph; however this stimulation would be the realistic consequence of fertilizer application anyway. For natural ecosystems, tracer is usually added to target a small ^{15}N enrichment $\boldsymbol{a_p}$ of the soil nitrate pool, like 5% in the case of Kulkarni et al. (2014). As will be shown in part 4.2 of this study, the use of a ^{15}N tracer does not always guarantee a perfect sensitivity and measurements are often below the limit of detection of the IRMS. It is thus desirable to inject as much tracer as possible without stimulating denitrification.

4. Recommendations for addressing technical challenges

4.1. Tracer application methods

Different methods of tracer application have been used in the past, such as injection through a syringe, application using a watering can or via a sprayer, as reviewed by Berendt et al. (2020). As shown in the same study, none of these three methods achieves perfect homogenisation of the tracer in the soil and losses are inevitable. The authors indeed found a theoretical ^{15}N enrichment of 57–59% in the upper 2.5 cm and 26–57% in 5–10 cm when targeting a 60% enrichment using a Bromide (Br^-) tracer. This is particularly relevant as in the ^{15}NGF, the tracer is also an anion (NO_3^-) and can therefore move more freely in the soil solution than a cation, which would rather remain in the upper layers. In the same study, distribution of the tracer is also shown to be more homogenised in dry soils. Application using a syringe can be challenging if they get clogged, however, this problem can be solved by using a metal wire inside the needle (obturator) as in Davidson et al. (1991).

Lewicka-Szczebak and Well (2020a) studied in detail the injection approach through three different methods; injection into an intact core (I + I), injection into a homogenised core (H + I) or mixed into a homogenised core (H + M). Obviously, the advantage of using the ^{15}NGF is to perform measurements directly *in situ*, which means that only the I + I approach is useable in the field. It was found that the determined N_2 fluxes and the denitrification product ratios did not differ significantly between intact and homogenised cores. Similarly, although soil properties are more homogeneous in mixed cores, it appears that the ^{15}N label is actually more evenly distributed in the I + I treatment. Notably, within the I + I treatment, the measured values of $\boldsymbol{a_p}$ from the gas emissions are closer to the determined ^{15}N abundance of the soil nitrate $\boldsymbol{a_{NO3}}$.

When choosing the injection method, the best way to homogenize the distribution of the tracer is to define a grid on the surface of the incubated soil and to use several injections of equal volume at different depths (Davidson et al., 1991; Tauchnitz et al., 2015; Sgouridis et al., 2016; Lewicka-Szczebak and Well, 2020a). Wu et al. (2011) determined in their experiments that the best compromise was 38 injections at 4 different depths. Buchen et al. (2016) used a more sophisticated system using a peristaltic pump and steel capillaries for better distribution of the tracer.

Finally, it is important to remember that since the tracer is diluted in water, injections will increase the soil moisture, which in turn will stimulate denitrification (Jarvis et al., 1991; Hwang and Hanaki, 2000). Usually, a soil moisture increase inferior to 3–5% is considered reasonable (Buchen et al., 2016; Sgouridis et al., 2016).

4.2. Sensitivity of the ^{15}NGF and use of a N_2-depleted atmosphere

The N_2 emitted from denitrification is challenging to measure and even the use of a ^{15}N tracer does not always guarantee a good signal on the IRMS. In cause is the sensitivity needed to detect the small amounts of produced N_2 against the high atmospheric N_2 background. Baily et al. (2012) reported the same limits of detection as Stevens and Laughlin (2001) on their IRMS, which were 8.0×10^{-6} for R29 and 3.2×10^{-7} for R30. Sgouridis et al. (2016) reported 7.7×10^{-7} for R29 and 6.1×10^{-7} for R30 while Friedl et al. (2017) reported 9.1×10^{-7} for R29 and 9.8×10^{-7} for R30. A simulation using Excel (Microsoft, Redmond, WA) has been used to determine how these limits of detection translate in terms of coefficients $\boldsymbol{d}$ that can be measured for a conventional use of the ^{15}NGF. Considering a 4 L incubation chamber, the ideal gas law and atmospheric pressure, different realistic values of $\boldsymbol{a_p}$ (ranging from 5% to 50%) and $\boldsymbol{d}$ (ranging from 1.10^{-8} to 5.10^{-4}) were used to calculate the associated ΔR29 and ΔR30, assuming isotopic equilibrium of the atmospheric and soil denitrifying pools. The values of $\boldsymbol{d}$ were translated into theoretical gas fluxes for informal reference, considering a 0.05 m^2 basal area of the incubation chamber and a time of incubation of 1 h. The results are reported in Table 4. The values of ΔR29 and ΔR30 that were

Table 5
Effect of N_2 background reduction on sensitivity.

d	Flux (gN/ha/d)	$[N_2]$ Atmospheric Background	$[N_2]$ = 20%	$[N_2]$ = 10%	$[N_2]$ = 5%	$[N_2]$ = 1%
		ΔR29	ΔR29	ΔR29	ΔR29	ΔR29
1E-08	0.19	3.18E-09	2.48E-09	2.48E-08	4.95E-08	2.48E-07
5E-08	0.94	1.59E-08	6.19E-08	1.24E-07	2.48E-07	1.24E-06
1E-07	1.88	3.18E-08	1.24E-07	2.48E-07	4.95E-07	2.48E-06
5E-07	9.36	1.59E-07	6.19E-07	1.24E-06	2.48E-06	1.24E-05
1E-06	18.74	3.18E-07	1.24E-06	2.48E-06	4.95E-06	2.48E-05
5E-06	93.6	1.59E-06	6.19E-06	1.24E-05	2.48E-05	1.24E-04
1E-05	187.4	3.18E-06	1.24E-05	2.48E-05	4.95E-05	2.48E-04
5E-05	936	1.59E-05	6.19E-05	1.24E-04	2.48E-04	1.24E-03
1E-04	1874	3.18E-05	1.24E-04	2.48E-04	4.95E-04	2.47E-03
5E-04	9366	1.59E-04	6.19E-04	1.24E-03	2.47E-03	1.21E-02

a) Comparison of ΔR29 with different N_2 backgrounds (cases where $\boldsymbol{a_p} = 20\%$) as calculated by simulation of a 4L chamber, assuming atmospheric pressure, the ideal gas law and isotopic equilibrium of the atmospheric and soil denitrifying pools. The ΔR29 ratios tend to be more detectable with lower N_2 background. Values in red cannot be detected with routinely available IRMS whereas values in yellow can be detected with higher resolution instruments. Values in green can be detected.
Colour code: ΔR29: Red $< 9.1 \times 10^{-7} <$ Yellow $< 8.0 \times 10^{-6} <$ Green
ΔR30: Red $< 3.2 \times 10^{-7} <$ Yellow $< 9.8 \times 10^{-7} <$ Green
Values of $\boldsymbol{d}$ are defined against atmospheric background. Fluxes values are given as informal example considering a 1-h incubation and a chamber basal area of 0.05 m^2.
b) Evolution and comparison of G29 and G30 ratios (see equation [10a] in part 4.2 of this study) with different N_2 backgrounds for the cases where $\boldsymbol{a_p} = 20\%$. We can see that G29 and G30 are identical for every similar situation (identical parameters $\boldsymbol{a_p}$, $\boldsymbol{d}$ and $[N_2]$ background). Furthermore, these ratios are almost invariant with $\boldsymbol{d}$ (nor with $\boldsymbol{a_p}$ as shown in **Annex 2**, **Supporting Information**).

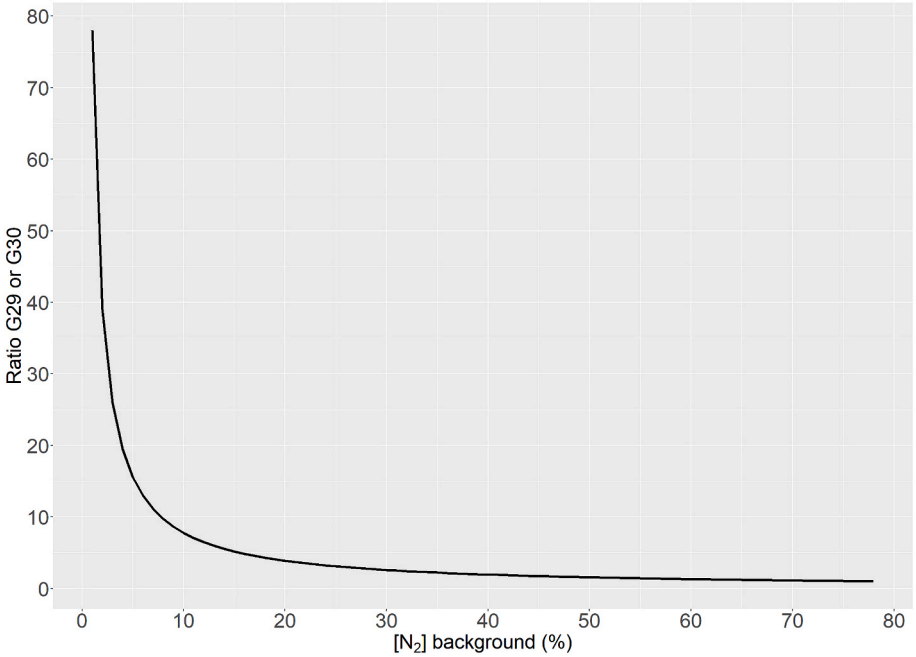

Fig. 7. Evolution of G_{29} (or G_{30}) with a background of $[N_2]$ ranging from 78% to 1% with an increment of 1%, as calculated through simulation. Maximum is $G_{29} = 78$ when $[N_2] = 1\%$. Minimum is $G_{29} = 1$ when $[N_2] = 78\%$.

beneath the smallest cited limit of detection appear in red, while the values greater than the highest cited limit of detection appear in green. The values in between are in yellow. This means that the values in red probably cannot be detected with the current routinely available technology whereas the values in yellow can only be detected if the IRMS has a good sensitivity. As expected, ΔR29 and ΔR30 tend to be more detectable when increasing both $\boldsymbol{a_p}$ and $\boldsymbol{d}$. Unfortunately, they are not detectable in most cases. Typically, $\boldsymbol{d}$ is rarely superior to 1.10^{-6}, which is not detectable even at a high ^{15}N abundance (50%) of the soil denitrifying pool. In addition, values in green in the simulation are only just above the detection limit in most cases, which is not ideal for accurate measurements. It is not rare to have gaps in a dataset of N_2 measurements because of this poor sensitivity (Mulvaney and Kurtz, 1984; Kulkarni et al., 2014; Buchen et al., 2016 amongst others; acknowledged by Friedl et al., 2020 as one of the main challenges of the ^{15}NGF).

One way to improve this sensitivity is to only use the R29 data in combination with the ^{15}N abundance $\boldsymbol{a_p}$ calculated through the N_2O data, as explained in section 2.2.3 of this study. Using this method, Baily et al. (2012) reported a sensitivity 16 times greater than when calculating $\boldsymbol{a_p}$ from the N_2 data. In order to optimize the R29 ratio, a 50% ^{15}N enrichment of the soil denitrifying pool represents an ideal target. Indeed, for a pool of N_2 at isotopic equilibrium, this is the enrichment for which the proportion of $^{29}N_2$ is the highest (equations [2a] to [2c]) as shown on Fig. 6.

If no denitrification stimulation occurs, targeting a 50% ^{15}N enrichment of the soil denitrifying pool is a good way to increase sensitivity.

Another way to increase sensitivity is to use a hybrid method as mentioned previously. More precisely, it means using an N_2-depleted atmosphere in addition to ^{15}N tracer. This new atmosphere should still contain a small amount of N_2 since the calculations of the ^{15}NGF require an [N_2] background. Similarly to Table 4, we can calculate the new ΔR29 and ΔR30 if the atmospheric background contains less N_2. We took the same cases as before ($\boldsymbol{a_p}$ ranging from 5% to 50% and $\boldsymbol{d}$ ranging from 1.10^{-8} to 5.10^{-4}) but now with a variable [N_2] background that contains either 78% (atmospheric), 20%, 10%, 5% or 1% of N_2 (see Table S6 in **Annex 2**, **Supporting Information**). The results for the case where $\boldsymbol{a_p}$ equals 20% can be seen in Table 5a (ΔR29 only, for clarity) and show as expected that ΔR29 tends to be more easily detected as the N_2 background drops. For identical values of $\boldsymbol{a_p}$ and $\boldsymbol{d}$, we can express the ratio G_{29} (and G30 similarly for ΔR30) defined as:

$$G_{29} = \frac{\Delta R29\ (\text{low } N_2 \text{ background})}{\Delta R29\ (\text{atmospheric } N_2 \text{ background})} \quad [10a]$$

If this ratio equals 4 (as it is approximately the case when $\boldsymbol{d} = 5.10^{-8}$, $\boldsymbol{a_p}$ = 20%, and [N_2] = 20%), then the limit of detection is increased 4 times. These ratios are compiled in Table 5b for the case $\boldsymbol{a_p}$ = 20%. Upon inspection of this table, it appears that G_{29} and G_{30} are equal for every identical situation (same parameters $\boldsymbol{d}$, $\boldsymbol{a_p}$ and [N_2] background). Furthermore, the values of G_{29} and G_{30} do not seem to depend significantly on the values of $\boldsymbol{d}$ and $\boldsymbol{a_p}$. This is demonstrated in **Annex 2** (**Supporting Information**) and therefore; much like Fig. 4, we can extrapolate a specific case (here we used $\boldsymbol{d} = 5.10^{-7}$ and $\boldsymbol{a_p}$ = 50%) to plot the evolution of the ratio G29 (equal to G30) as a function of the [N_2] background for every scenario. Fig. 7 represents this evolution:

We can see from Fig. 7 that no matter the quantity of tracer applied or the number of molecules emitted, the sensitivity significantly increases when the background in [N_2] < 10%. It is approximately enhanced 10 times when [N_2] = 8%. If the background drops below 1%, even better sensitivity can be obtained; for example, G_{29} is equal to 156 and 780 when the [N_2] background reaches 0.5% and 0.1%, respectively. It can be very challenging to maintain these low levels of N_2 however, even in the laboratory as can be seen in Well et al. (2019a). As mentioned in section 1 of this study, this method has not been used extensively because of its complexity (laboratory studies: Meyer et al., 2010; Scheer et al., 2016; Lewicka-Szczebak et al., 2017; Lewicka-Szczebak and Well, 2020a; Kemmann et al., 2021; *in situ* studies: Well et al., 2019a; Buchen-Tschiskale et al., 2023).

Finally, it is important to remember that R29 and R30 after incubation are necessarily greater than their initial values, as shown in **Annex 3** (**Supporting Information**). Therefore, any value of R29 or R30 after incubation lower than its initial value can only be noise from the IRMS and cannot give any realistic value.

Similarly, it is also worth noting that $(R29)_0$ and $(R30)_0$ are supposedly constant and equal to 7.35×10^{-3} and 1.35×10^{-5}, respectively. These values are easily found using a binomial distribution with a ^{15}N enrichment equal to natural abundance $\boldsymbol{a_a}$ (~0.37%):

$$R29_{(0)} = \frac{2 \times 0.003663 \times (1 - 0.003663)}{(1 - 0.003663)^2} = 7.35 \times 10^{-3} \quad [10b]$$

$$R30_{(0)} = \frac{0.003663^2}{(1 - 0.003663)^2} = 1.35 \times 10^{-5} \quad [10c]$$

Thus, a good way to calibrate the IRMS is to perform tests on atmospheric samples and try to find these values as in Lewicka-Szczebak et al. (2013). Care must be taken for m/z = 30 as shown next.

4.3. Interferences at m/z = 30 and gas-purification preparation unit

If trace amounts of oxygen are present in the ion source of the IRMS, various species with m/z = 30 can be formed; such as $(^{13}C^{17}O)^+$, $(^{12}C^{18}O)^+$ or $(^{14}N^{16}O)^+$ (Russow et al., 1996). It has been suggested that the removal of hindering gaseous species such as H_2O, CO_2, CO and N_2O (the last one only when studying N_2) would allow for a better sensitivity (Lewicka-Szczebak et al., 2013). Siegel et al. (1982) were the first ones to develop a gas-purification preparation unit for the use of the ^{15}NGF. More recently, such systems were also developed and used by Lewicka-Szczebak et al. (2013), Yang et al. (2014) and Sgouridis et al. (2016).

However, this usually does not solve entirely the problem as shown by the results in Table 2 from Lewicka-Szczebak et al. (2013); where R30 from the atmosphere is approximately 10 times greater than the expected value. As explained in the same study, the magnitude of NO^+ formed in the ion source of the IRMS depends on the quantity of injected N_2. Thus, the authors applied a drift correction as a linear function of $^{28}N_2$. Russow et al. (1996) solved this problem more directly by using standards and a linear drift correction as:

$$R30_{true} = a \times R30_{measured} + b \quad [11a]$$

Excellent correlation was obtained ($R^2 = 1$) and the coefficient $\boldsymbol{a}$ in their case was close to 1. This means that calculations based on ΔR30 such as the ones from Mulvaney and Boast (1986) would still give a good result without correction. However, the equations based on the approach of Arah (1992) would lead to error given that R30 in the following equations would not have been corrected:

$$a_m = \frac{R_{29} + 2R_{30}}{2(1 + R_{29} + R_{30})} \quad [11b]$$

$$\alpha_m = \frac{R_{30}}{1 + R_{29} + R_{30}} \quad [11c]$$

Modern ultrahigh resolution mass spectrometers can separate $^{14}N^{16}O$ from $^{30}N_2$ (Yeung et al., 2017, 2019) but these instruments are not routinely available and current sample throughput is limited due to an analysis time of a few hours per sample.

Finally, it is worth mentioning that in the past, some authors have avoided the issue at m/z = 30 by isotopically equilibrating the mix of emitted and atmospheric N_2 through high voltage arc, electrodeless discharge or microwave equilibration (Well et al., 1998). These techniques have been of little use lately because it required two runs per sample and modern IRMS have a better sensitivity towards $^{30}N_2$.

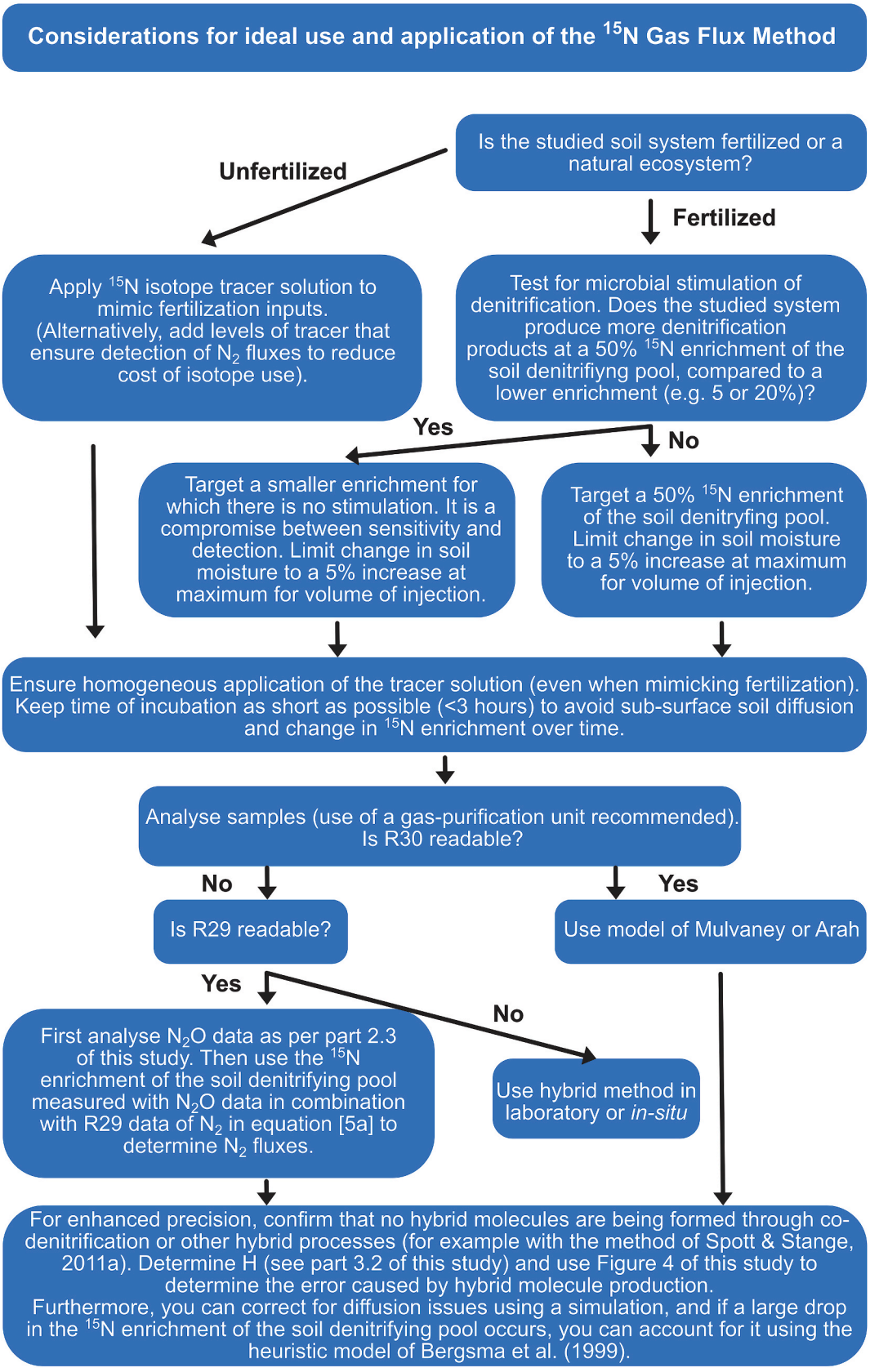

Fig. 8. Decision tree of the considerations for an ideal use and application of the ^{15}NGF.

5. Conclusion and future research

The ^{15}NGF method remains today, the most suitable technique for studying denitrification *in situ* in soil. However, its results can be biased by different factors as shown here, especially the non-homogeneous distribution of the label in the soil, the formation of hybrid molecules, the diffusion issues and the addition of substrate labelled tracer. The non-homogeneous distribution of the label and the diffusion issues tend to result in an underestimation of the true potential of denitrification. On the other hand, the potential stimulation of denitrification due to substrate addition and the eventual formation of hybrid molecules would tend to overestimate it. We demonstrate herein that a better precision in the measurement of denitrification can be obtained by:

1) Ensuring the most homogeneous label application so that the soil denitrifying pool is as close as possible to isotopic equilibrium as originally presumed in the ^{15}NGF method.
2) Accounting for diffusion by allowing time after label application in order to reach near-steady-state profiles of gas concentration and diffusive fluxes; and using a simulation to calculate storage and subsoil fluxes. Alternatively, the use of a bottom-closed cylinder in the field can also be a viable option although it leads to soil and root system disturbances.
3) Define a level of tracer addition that reduces and/or eliminate denitrification stimulation.
4) Check if hybrid processes are occurring in the type of soil system studied.

A preparation unit for gas purification is also very valuable but does not entirely solve the problems that occur at m/z = 30. A drift correction might still be needed.

Furthermore, because the atmospheric N_2 background is so high and denitrification can emit very small amounts of N_2, sensitivity might still not be sufficient to quantify denitrification beyond peak events. The only experimental parameters one can modify to increase sensitivity are the time of incubation, the size of the headspace inside the incubation vessel, the amount of ^{15}N label used (optimizing the ^{15}N enrichment of the nitrate pool) and the level of N_2 concentration in the atmospheric background. Increasing the time of incubation and decreasing the size of the headspace can both increase sensitivity but they will also cause further diffusion issues when using the ^{15}NGF *in situ*. Labelling 50% of the soil denitrifying pool represents an ideal target to increase sensitivity towards R29. If no denitrification stimulation occurs at this level, this is a good way to increase sensitivity. The reduction of the N_2 atmospheric background *in situ* can be challenging, given that it requires a tightly sealed incubation chamber system and that air can still circulate through soil pores. Nonetheless, this was achieved recently by Well et al. (2019a) using a sophisticated incubation and soil flushing system. However, this method is difficult to use at a wider scale and is not appropriated for intensive sampling campaigns. It is not necessary to get rid of all the native atmospheric N_2, reducing it to a lower and known concentration (~<10%) can already increase sensitivity significantly. To help users in the successful application of the ^{15}NGF, we have summarized our conclusions into a decision tree (see Fig. 8).

It will need further work and innovation to further increase the sensitivity of the ^{15}NGF and allow robust and reproducible measurements of field denitrification in the future.

Declaration of competing interest

The authors declare that they have no known competing financial interests or personal relationships that could have appeared to influence the work reported in this paper.

Data availability

Data will be made available on request.

Acknowledgements

The authors acknowledge funding from the BBSRC Sustainable Agriculture Research and Innovation Club project (BB/R021716/1) and from the U.K. Natural Environment Research Council (NERC grant NE/S007350/1). The authors are grateful to The Allerton Project Game & Wildlife Conservation Trust (Loddington, U.K.) for their collaboration and permission to access their land to sample soil.

Appendix A. Supplementary data

Supplementary data to this article can be found online at https://doi.org/10.1016/j.soilbio.2023.109108.

References

Almaraz, M., Wong, M.Y., Yang, W.H., 2020. Looking back to look ahead: a vision for soil denitrification research. Ecology 101 (1). https://doi.org/10.1002/ecy.2917.

Anthony, W.H., Hutchinson, G.L., Livingston, G.P., 1995. Chamber measurement of soil-atmosphere gas exchange : linear vs. Diffusion-based flux models. Soil Science Society of America Journal 59 (5), 1308–1310. https://doi.org/10.2136/sssaj1995.03615995005900050015x.

Arah, J.R.M., 1992. New formulae for mass spectrometric analysis of nitrous oxide and dinitrogen emissions. Soil Science Society of America Journal 56 (3), 795–800. https://doi.org/10.2136/sssaj1992.03615995005600030020x.

Arah, J.R.M., Crichton, I.J., Smith, K.A., 1993. Denitrification measured directly using a single-inlet mass spectrometer and by acetylene inhibition. Soil Biology and Biochemistry 25 (Issue 2), 233–238. https://doi.org/10.1016/0038-0717(93)90032-7.

Arah, J.R.M., 1997. Apportioning nitrous oxide fluxes between nitrification and denitrification using gas-phase mass spectrometry. Soil Biology and Biochemistry 29 (Issue 8), 1295–1299. https://doi.org/10.1016/S0038-0717(97)00027-8.

Baily, A., Watson, C.J., Laughlin, R., Matthews, D., McGeough, K., Jordan, P., 2012. Use of the ^{15}N gas flux method to measure the source and level of N_2O and N_2 emissions from grazed grassland. Nutrient Cycling in Agroecosystems 94 (2–3), 287–298. https://doi.org/10.1007/s10705-012-9541-x.

Berendt, J., Tenspolde, A., Rex, D., Clough, T.J., Wrage-Mönnig, N., 2020. Application methods of tracers for N_2O source determination lead to inhomogeneous distribution in field plots. Analytical Science Advances 1 (4), 221–232. https://doi.org/10.1002/ansa.202000100.

Bergsma, T.T., Bergsma, Q.C., Ostrom, N.E., Robertson, G.P., 1999. A heuristic model for the calculation of dinitogen and nitrous oxide flux from nitrogen-15-labeled soil. Soil Science Society of America Journal 63 (6), 1709–1716. https://doi.org/10.2136/sssaj1999.6361709x.

Bergsma, T.T., Ostrom, N.E., Emmons, M., Robertson, G.P., 2001. Measuring simultaneous fluxes from soil of N_2O and N_2 in the field using the ^{15}N-gas "nonequilibrium" technique. Environmental Science and Technology 35 (21), 4307–4312. https://doi.org/10.1021/es010885u.

Boast, C.W., Mulvaney, R.L., Baveye, P., 1988. Evaluation of nitrogen-15 tracer techniques for direct measurement of denitrification in soil: I. Theory. Soil Science Society of America Journal 52 (5), 1317–1322. https://doi.org/10.2136/sssaj1988.03615995005200050020x.

Bollmann, A., Conrad, R., 1997. Acetylene blockage technique leads to underestimation of denitrification rates in oxic soils due to scavenging of intermediate nitric oxide. Soil Biology and Biochemistry 29 (Issue 7), 1067–1077. https://doi.org/10.1016/S0038-0717(97)00007-2.

Bremner, J.M., 1997. Sources of nitrous oxide in soils. In: Nutrient Cycling in Agroecosystems, 49. Kluwer Academic Publishers. https://doi.org/10.1023/A:1009798022569.

Buchen, C., Lewicka-Szczebak, D., Fuß, R., Helfrich, M., Flessa, H., Well, R., 2016. Fluxes of N_2 and N_2O and contributing processes in summer after grassland renewal and grassland conversion to maize cropping on a Plaggic Anthrosol and a Histic Gleysol. Soil Biology and Biochemistry 101, 6–19. https://doi.org/10.1016/j.soilbio.2016.06.028.

Buchen-Tschiskale, C., Well, R., Flessa, H., 2023. Tracing nitrogen transformations during spring development of winter wheat induced by ^{15}N labeled cattle slurry applied with different techniques. Science of the Total Environment 871 (February), 162061. https://doi.org/10.1016/j.scitotenv.2023.162061.

Butterbach-Bahl, K., Willibald, G., Papen, H., 2002. Soil core method for direct simultaneous determination of N_2 and N_2O emissions from forest soils. Plant and Soil 240 (No. 1), 105–116. https://doi.org/10.1023/A:1015870518723.

Cárdenas, L.M., Hawkins, J.M.B., Chadwick, D., Scholefield, D., 2003. Biogenic gas emissions from soils measured using a new automated laboratory incubation system. Soil Biology and Biochemistry 35 (Issue 6), 867–870. https://doi.org/10.1016/S0038-0717(03)00092-0.

Cho, C.M., Sakdinan, L., 1978. Mass spectrometric investigation on denitrification. Canadian Journal of Soil Science 58 (3), 443–457. https://doi.org/10.4141/cjss78-051.

Clayton, H., Mctaggart, I.P., Parker, J., Swan, L., Smith, K.A., Smith, K.A., 1997. Nitrous oxide emissions from fertilised grassland: a 2-year study of the effects of N fertiliser form and environmental conditions. Biology and Fertility of Soils 25, 252–260. https://doi.org/10.1007/s003740050311 nº 3.

Clough, T.J., Stevens, R.J., Laughlin, R.J., Sherlock, R.R., Cameron, K.C., 2001. Transformations of inorganic-N in soil leachate under differing storage conditions. Soil Biology and Biochemistry 33 (Issue 11), 1473–1480. https://doi.org/10.1016/S0038-0717(01)00056-6.

Clough, T.J., Sherlock, R.R., Rolston, D.E., 2005. A review of the movement and fate of N_2O in the subsoil. Nutrient Cycling in Agroecosystems 72 (1), 3–11. https://doi.org/10.1007/s10705-004-7349-z.

Clough, T.J., Lanigan, G.J., de Klein, C.A.M., Samad, M.S., Morales, S.E., Rex, D., Bakken, L.R., Johns, C., Condron, L.M., Grant, J., Richards, K.G., 2017. Influence of soil moisture on codenitrification fluxes from a urea-affected pasture soil. Scientific Reports 7 (1). https://doi.org/10.1038/s41598-017-02278-y.

Cuhel, J., Simek, M., Laughlin, R.J., Bru, D., Chèneby, D., Watson, C.J., Philippot, L., 2010. Insights into the effect of soil pH on N_2O and N_2 emissions and denitrifier community size and activity. Applied and Environmental Microbiology 76 (6), 1870–1878. https://doi.org/10.1128/AEM.02484-09.

Davidson, E.A., Hart, S.C., Shanks, C.A., Firestone, M.K., 1991. Measuring gross nitrogen mineralization, and nitrification by ^{15}N isotopic pool dilution in intact soil cores. Journal of Soil Science 42, 335–349. https://doi:10.1111/j.1365-2389.1991.tb00413.x.

Deppe, M., Well, R., Giesemann, A., Spott, O., Flessa, H., 2017. Soil N_2O fluxes and related processes in laboratory incubations simulating ammonium fertilizer depots. Soil Biology and Biochemistry 104, 68–80. https://doi.org/10.1016/j.soilbio.2016.10.005.

Dodds, W.K., Burgin, A.J., Marcarelli, A.M., Strauss, E.A., 2017. Nitrogen transformations. In: Methods in Stream Ecology, third ed. (Vol. 2. Elsevier, pp. 173–196. https://doi.org/10.1016/B978-0-12-813047-6.00010-3.

Focht, D.D., Stolzy, L.H., 1978. Long-term denitrification studies in soils fertilized with $(^{15}NH_4)_2SO_4$. Soil Science Society of America Journal 42, 894–898. https://doi.org/10.2136/sssaj1978.03615995004200060012x.

Focht, D.D., Stolzy, L.H., Meek, B.D., 1979. Sequential reduction of nitrate and nitrous oxide under field conditions as brought about by organic amendments and irrigation management. Soil Biology and Biochemistry 11 (Issue 1), 37–46. https://doi.org/10.1016/0038-0717(79)90116-0.

Focht, D.D., Valoras, N., Letey, J., 1980. Use of interfaced gas chromatography-mass spectrometry for detection of concurrent mineralization and denitrification in soil. Journal of Environmental Quality 9, 218–223. https://doi.org/10.2134/jeq1980.00472425000900020011x nº 2.

Forthofer, R.N., Lee, E.S., Hernandez, M., 2007. Linear regression. In: Biostatistics. Elsevier, pp. 349–386. https://doi.org/10.1016/B978-0-12-369492-8.50018-2.

Friedl, J., Scheer, C., Rowlings, D.W., Mumford, M.T., Grace, P.R., 2017. The nitrification inhibitor DMPP (3,4-dimethylpyrazole phosphate) reduces N_2 emissions from intensively managed pastures in subtropical Australia. Soil Biology and Biochemistry 108, 55–64. https://doi.org/10.1016/j.soilbio.2017.01.016.

Friedl, J., Cardenas, L.M., Clough, T.J., Dannenmann, M., Hu, C., Scheer, C., 2020. Measuring denitrification and the N_2O:($N_2O + N_2$) emission ratio from terrestrial soils. Current Opinion in Environmental Sustainability 47, 61–71. https://doi.org/10.1016/j.cosust.2020.08.006. Elsevier B.V.

Groffman, P.M., Tiedje, J.M., 1989. Denitrification in north temperate forest soils: spatial and temporal patterns at the landscape and seasonal scales. Soil Biology and Biochemistry 21 (Issue 5), 613–620. https://doi.org/10.1016/0038-0717(89)90053-9.

Groffman, P.M., Altabet, M.A., Böhlke, J.K., Butterbach-Bahl, K., David, M.B., Firestone, M.K., Giblin, A.E., Kana, T.M., Nielsen, L.P., Voytek, M.A., 2006. Methods for measuring denitrification: diverse approaches to a difficult problem. Ecological Applications 16 (Issue 6). https://doi.org/10.1890/1051-0761(2006)016, 2091: MFMDDA]2.0.CO;2.

Guiraud, G., Berlier, Y.(, 1970. Quantitative and isotopic determination by mass spectrometry of gaseous compounds produced during denitrification. Chimie Analytique 52, 53–56.

Hauck, R.D., Melsted, S.W., 1956. Some aspects of the problem of evaluating denitrification in soils. Soil Science Society of America Journal 20 (3), 361–364. https://doi.org/10.2136/sssaj1956.03615995002000030017x.

Hauck, R.D., Melsted, S.W., Yankwich, P.E., 1958. Use of N-isotope distribution in nitrogen gas in the study of denitrification. Soil Science 86, 287. https://doi.org/10.1097/00010694-195811000-00011.

Hauck, R., Bouldin, D., 1961. Distribution of isotopic nitrogen in nitrogen gas during denitrification. Nature 191, 871–872. https://doi.org/10.1038/191871a0.

Hayes, J.M., 1993. In: Meinschein, W.G. (Ed.), Organic Geochemistry of Contemporaneous and Ancient Sediments. Society of Economic Paleontologists and Minerologists, Bloomington, 5-1.

Hossler, K., Bouchard, V., 2008. The joint estimation of soil trace gas fluxes. Soil Science Society of America Journal 72 (5), 1382–1393. https://doi.org/10.2136/sssaj2007.0232.

Humbert, S., Tarnawski, S., Fromin, N., Mallet, M.P., Aragno, M., Zopfi, J., 2010. Molecular detection of anammox bacteria in terrestrial ecosystems: distribution and diversity. ISME Journal 4 (3), 450–454. https://doi.org/10.1038/ismej.2009.125.

Hutchinson, G.L., Mosier, A.R., 1981. Improved soil cover method for field measurement of nitrous oxide fluxes. Soil Science Society of America Journal 45 (2), 311–316. https://doi.org/10.2136/sssaj1981.03615995004500020017x.

Hutchinson, G.L., Livingston, G.P., 2002. 4.5 Soil–atmosphere gas exchange. In: Dane, J. H., Clarke Topp, G. (Eds.), Methods of Soil Analysis. https://doi.org/10.2136/sssabookser5.4.c47.

Hwang, S., Hanaki, K., 2000. Effects of oxygen concentration and moisture content of refuse on nitrification, denitrification and nitrous oxide production. Bioresource Technology 71 (2), 159–165. https://doi.org/10.1016/S0960-8524(99)90068-8.

IPCC, 2013. Climate change 2013: the physical science basis. In: Contribution of Working Group I to the Fifth Assessment Report of the Intergovernmental Panel on Climate Change. Rep., Cambridge, UK and New York, p. 1535.

Jarvis, S.C., Barraclough, D., Williams, J., Rook, A.J., 1991. Patterns of denitrification loss from grazed grassland: effects of N fertilizer inputs at different sites. Plant and Soil 131. https://doi.org/10.1007/BF00010422.

Jaynes, D.B., Rogowski, A.S., 1983. Applicability of Fick's law to gas diffusion. Soil Science Society of America Journal 47, 425–430. https://doi.org/10.2136/sssaj1983.03615995004700030007x.

Kemmann, B., Wöhl, L., Fuß, R., Schrader, S., Well, R., Ruf, T., 2021. N_2 and N_2O mitigation potential of replacing maize with the perennial biomass crop Silphium perfoliatum—an incubation study. GCB Bioenergy 13 (10), 1649–1665. https://doi.org/10.1111/gcbb.12879.

Krause, H.M., Thonar, C., Eschenbach, W., Well, R., Mäder, P., Behrens, S., Kappler, A., Gattinger, A., 2017. Long term farming systems affect soils potential for N_2O production and reduction processes under denitrifying conditions. Soil Biology and Biochemistry 114, 31–41. https://doi.org/10.1016/j.soilbio.2017.06.025.

Kulkarni, M.V., Burgin, A.J., Groffman, P.M., Yavitt, J.B., 2014. Direct flux and ^{15}N tracer methods for measuring denitrification in forest soils. Biogeochemistry 117 (2–3), 359–373. https://doi.org/10.1007/s10533-013-9876-7.

Lassaletta, L., Billen, G., Grizzetti, B., Anglade, J., Garnier, J., 2014. 50 year trends in nitrogen use efficiency of world cropping systems: the relationship between yield and nitrogen input to cropland. Environmental Research Letters 9 (10). https://doi.org/10.1088/1748-9326/9/10/105011.

Laughlin, R.J., Stevens, R.J., 2002. Evidence for fungal dominance of denitrification and codenitrification in a Grassland Soil. Soil Science Society of America Journal 66 (5), 1540–1548. https://doi.org/10.2136/sssaj2002.1540.

Laughlin, R.J., Stevens, R.J., 2003. Changes in composition of nitrogen-15-labeled gases during storage in septum-capped vials. Soil Science Society of America Journal 67, 540–543. https://doi.org/10.2136/sssaj2003.5400.

Lewicka-Szczebak, D., Well, R., Giesemann, A., Rohe, L., Wolf, U., 2013. An enhanced technique for automated determination of ^{15}N signatures of N_2, (N_2+N_2O) and N_2O in gas samples. Rapid Communications in Mass Spectrometry 27 (13), 1548–1558. https://doi.org/10.1002/rcm.6605.

Lewicka-Szczebak, D., Augustin, J., Giesemann, A., Well, R., 2017. Quantifying N_2O reduction to N_2 based on N_2O isotopocules - validation with independent methods (helium incubation and ^{15}N gas flux method). Biogeosciences 14 (3), 711–732. https://doi.org/10.5194/bg-14-711-2017.

Lewicka-Szczebak, D., Well, R., 2020a. The ^{15}N gas-flux method to determine N_2 flux: a comparison of different tracer addition approaches. SOIL 6 (1), 145–152. https://doi.org/10.5194/soil-6-145-2020.

Lewicka-Szczebak, D., Piotr Lewicki, M., Well, R., 2020b. N_2O isotope approaches for source partitioning of N_2O production and estimation of N_2O reduction-validation with the ^{15}N gas-flux method in laboratory and field studies. Biogeosciences 17 (22), 5513–5537. https://doi.org/10.5194/bg-17-5513-2020.

Liu, Y., Wang, R., Pan, Z.L., Zheng, X.H., Wei, H.H., Zhang, H.R., Mei, B.L., Quan, Z., Fang, Y.T., Ju, X.T., 2022. Quantifying in situ N_2 fluxes from an intensively managed calcareous soil using the ^{15}N gas-flux method. Journal of Integrative Agriculture 21 (9), 2750–2766. https://doi.org/10.1016/j.jia.2022.07.016.

Livingston, G.P., Hutchinson, G.L., Spartalian, K., 2006. Trace gas emission in chambers. Soil Science Society of America Journal 70 (5), 1459–1469. https://doi.org/10.2136/sssaj2005.0322.

Loick, N., Dixon, E.R., Abalos, D., Vallejo, A., Matthews, G.P., McGeough, K.L., Well, R., Watson, C.J., Laughlin, R.J., Cardenas, L.M., 2016. Denitrification as a source of nitric oxide emissions from incubated soil cores from a UK grassland soil. Soil Biology and Biochemistry 95, 1–7. https://doi.org/10.1016/j.soilbio.2015.12.009.

Loick, N., Dixon, E., Abalos, D., Vallejo, A., Matthews, P., McGeough, K., Watson, C., Baggs, E.M., Cardenas, L.M., 2017. "Hot spots" of N and C impact nitric oxide, nitrous oxide and nitrogen gas emissions from a UK grassland soil. Geoderma 305, 336–345. https://doi.org/10.1016/j.geoderma.2017.06.007.

Long, A., Heitman, J., Tobias, C., Philips, R., Song, B., 2013. Co-occurring anammox, denitrification, and codenitrification in agricultural soils. Applied and Environmental Microbiology 79 (1), 168–176. https://doi.org/10.1128/AEM.02520-12.

McGeough, K.L., Laughlin, R.J., Watson, C.J., Müller, C., Ernfors, M., Cahalan, E., Richards, K.G., 2012. The effect of cattle slurry in combination with nitrate and the nitrification inhibitor dicyandiamide on in situ nitrous oxide and dinitrogen emissions. Biogeosciences 9 (12), 4909–4919. https://doi.org/10.5194/bg-9-4909-2012.

Meyer, M.L., Bloom, P.R., Grava, J., 1989. Transformation and losses of applied nitrogen-15 labeled ammonium in a flooded organic soil. Soil Science Society of America Journal 53, 79–85. https://doi.org/10.2136/sssaj1989.03615995005300010015x.

Meyer, A., Bergmann, J., Butterbach-Bahl, K., Brüggemann, N., 2010. A new ^{15}N tracer method to determine N turnover and denitrification of Pseudomonas stutzeri. Isotopes in Environmental and Health Studies 46 (4), 409–421. https://doi.org/10.1080/10256016.2010.528840.

Morse, J.L., Bernhardt, E.S., 2013. Using ^{15}N tracers to estimate N_2O and N_2 emissions from nitrification and denitrification in coastal plain wetlands under contrasting land-uses. Soil Biology and Biochemistry 57, 635–643. https://doi.org/10.1016/j.soilbio.2012.07.025.

Müller, C., Laughlin, R.J., Spott, O., Rütting, T., 2014. Quantification of N_2O emission pathways via a ^{15}N tracing model. Soil Biology and Biochemistry 72, 44–54. https://doi.org/10.1016/j.soilbio.2014.01.013.

Mulvaney, R.L., Kurtz, L.T., 1982. A new method for determination of ^{15}N-labeled nitrous oxide. Soil Science Society of America Journal 46, 1178–1184. https://doi.org/10.2136/sssaj1982.03615995004600060012x nº 6.

Mulvaney, R.L., 1984. Determination of ^{15}N-labeled dinitrogen and nitrous oxide with triple-collector mass spectrometers. Soil Science Society of America Journal 48, 690–692. https://doi.org/10.2136/sssaj1984.03615995004800030045x.

Mulvaney, R.L., Kurtz, L.T., 1984. Evolution of dinitrogen and nitrous oxide from nitrogen-15 fertilized soil cores subjected to wetting and drying cycles. Soil Science Society of America Journal 48 (3), 596–602. https://doi.org/10.2136/sssaj1984.03615995004800030026x.

Mulvaney, R.L., Boast, C.W., 1986. Equations for determination of nitrogen-15 labeled dinitrogen and nitrous oxide by mass spectrometry. Soil Science Society of America Journal 50 (2), 360–363. https://doi.org/10.2136/sssaj1986.03615995005000020021x.

Mulvaney, R.L., 1988. Evaluation of nitrogen-15 tracer techniques for direct measurement of denitrification in soil: III. laboratory studies. Soil Science Society of America Journal 52 (5), 1327–1332. https://doi.org/10.2136/sssaj1988.03615995005200050022x.

Mulvaney, R.L., Vanden Heuvel, R.M., 1988. Evaluation of nitrogen-15 tracer techniques for direct measurement of denitrification in soil: IV. field studies. Soil Science Society of America Journal 52 (5), 1332–1337. https://doi.org/10.2136/sssaj1988.03615995005200050023x.

Myrold, D.D., 1990. Measuring denitrification in soils using 15N techniques. In: Revsbech, N.P., Sørensen, J. (Eds.), Denitrification in Soil and Sediment, Federation of European Microbiological Societies Symposium Series, 56. Springer, Boston, MA. https://doi.org/10.1007/978-1-4757-9969-9_11.

Nadeem, S., Dörsch, P., Bakken, L.R., 2013. Autoxidation and acetylene-accelerated oxidation of NO in a 2-phase system: implications for the expression of denitrification in ex situ experiments. Soil Biology and Biochemistry 57, 606–614. https://doi.org/10.1016/j.soilbio.2012.10.007.

Parkin, T.B., Venterea, R.T., Hargreaves, S.K., 2012. Calculating the detection limits of chamber-based soil greenhouse gas flux measurements. Journal of Environmental Quality 41 (3), 705–715. https://doi.org/10.2134/jeq2011.0394.

Pedersen, A.R., 2000. Estimating the nitrous oxide emission rate from the soil surface by means of a diffusion model. Scandinavian Journal of Statistics 27, 385–403. https://doi.org/10.1111/1467-9469.00196.

Pedersen, A.R., Petersen, S.O., Vinther, F.P., 2001. Stochastic diffusion model for estimating trace gas emissions with static chambers. Soil Science Society of America Journal 65 (1), 49–58. https://doi.org/10.2136/sssaj2001.65149x.

Pedersen, A.R., Petersen, S.O., Schelde, K., 2010. A comprehensive approach to soil-atmosphere trace-gas flux estimation with static chambers. European Journal of Soil Science 61 (6), 888–902. https://doi.org/10.1111/j.1365-2389.2010.01291.x.

Phillips, R.L., Song, B., McMillan, A.M.S., Grelet, G., Weir, B.S., Palmada, T., Tobias, C., 2016. Chemical formation of hybrid di-nitrogen calls fungal codenitrification into question. Scientific Reports 6. https://doi.org/10.1038/srep39077.

Ravishankara, A.R., Daniel, J.S., Portmann, R.W., 2009. Nitrous oxide (N_2O): the dominant ozone-depleting substance emitted in the 21st century. Science 326 (5949), 123–125. https://doi.org/10.1126/science.1176985.

Rohe, L., Anderson, T.H., Flessa, H., Goeske, A., Lewicka-Szczebak, D., Wrage-Mönnig, N., Well, R., 2021. Comparing modified substrate-induced respiration with selective inhibition (SIRIN) and N_2O isotope approaches to estimate fungal contribution to denitrification in three arable soils under anoxic conditions. Biogeosciences 18 (15), 4629–4650. https://doi.org/10.5194/bg-18-4629-2021.

Rolston, D.E., Hoffman, D.L., Toy, D.W., 1978. Field measurement of denitrification: I. Flux of N_2 and N_2O. Soil Science Society of America Journal 42, 863–869. https://doi.org/10.2136/sssaj1978.03615995004200060004x.

Rolston, D.E., Sharpley, A.N., Toy, D.W., Broadbent, F.E., 1982. Field measurement of denitrification: III. Rates during irrigation cycles. Soil Science Society of America Journal 46, 289–296. https://doi.org/10.2136/sssaj1982.03615995004600020015x.

Rummel, P.S., Well, R., Pfeiffer, B., Dittert, K., Floßmann, S., Pausch, J., 2021. Nitrate uptake and carbon exudation – do plant roots stimulate or inhibit denitrification? Plant and Soil 459 (1–2), 217–233. https://doi.org/10.1007/s11104-020-04750-7.

Ruser, R., Flessa, H., Russow, R., Schmidt, G., Buegger, F., Munch, J.C., 2006. Emission of N_2O, N_2 and CO_2 from soil fertilized with nitrate: effect of compaction, soil moisture and rewetting. Soil Biology and Biochemistry 38 (Issue 2), 263–274. https://doi.org/10.1016/j.soilbio.2005.05.005.

Russow, R., Stevens, R.J., Laughlin, R.J., 1996. Accuracy and precision for measurements of the mass ratio 30/28 in dinitrogen from air samples and its application to the investigation of N losses from soil by denitrification. Isotopes in Environmental and Health Studies 32 (2–3), 289–297. https://doi.org/10.1080/10256019608036322.

Saggar, S., Jha, N., Deslippe, J., Bolan, N.S., Luo, J., Giltrap, D.L., Kim, D.G., Zaman, M., Tillman, R.W., 2013. Denitrification and N_2O: N_2 production in temperate grasslands: processes, measurements, modelling and mitigating negative impacts. Science of the Total Environment 465, 173–195. https://doi.org/10.1016/j.scitotenv.2012.11.050.

Scheer, C., Meier, R., Brüggemann, N., Grace, P.R., Dannenmann, M., 2016. An improved ^{15}N tracer approach to study denitrification and nitrogen turnover in soil incubations. Rapid Communications in Mass Spectrometry : Rapid Communications in Mass Spectrometry 30 (18), 2017–2026. https://doi.org/10.1002/rcm.7689.

Seitzinger, S.P., Nielsen, L.P., Caffrey, J., Christensen, P.B., 1993. Denitrification measurements in aquatic sediments: a comparison of three methods. Biogeochemistry 23 (3), 147–167. http://www.jstor.org/stable/1469044.

Seitzinger, S., Harrison, J.A., Böhlke, J.K., Bouwman, A.F., Lowrance, R., Peterson, B., Tobias, C., Drecht, G.V., 2006. Denitrification across landscapes and waterscapes : a synthesis. Ecological Applications 16 (6), 2064–2090. https://doi.org/10.1890/1051-0761(2006)016[2064:DALAWA]2.0.CO, 2.

Selbie, D.R., Lanigan, G.J., Laughlin, R.J., Di, H.J., Moir, J.L., Cameron, K.C., Clough, T. J., Watson, C.J., Grant, J., Somers, C., Richards, K.G., 2015. Confirmation of co-denitrification in grazed grassland. Scientific Reports 5. https://doi.org/10.1038/srep17361.

Sgouridis, F., Ullah, S., 2015. Relative magnitude and controls of in Situ N_2 and N_2O fluxes due to denitrification in natural and seminatural terrestrial ecosystems using ^{15}N tracers. Environmental Science and Technology 49 (24), 14110–14119. https://doi.org/10.1021/acs.est.5b03513.

Sgouridis, F., Stott, A., Ullah, S., 2016. Application of the ^{15}N gas-flux method for measuring in situ N_2 and N_2O fluxes due to denitrification in natural and semi-natural terrestrial ecosystems and comparison with the acetylene inhibition technique. Biogeosciences 13 (6), 1821–1835. https://doi.org/10.5194/bg-13-1821-2016.

Shoun, H., Kim, D.-H., Uchiyama, H., Sugiyama, J., 1992. Denitrification by fungi. FEMS Microbiology Letters 94 (3), 277–281. https://doi.org/10.1111/j.1574-6968.1992.tb05331.x.

Siegel, R.S., Hauck, R.D., Kurtz, L.T., 1982. Determination of $^{30}N_2$ and application to measurement of N_2 evolution during denitrification. Soil Science Society of America Journal 46, 68–74. https://doi.org/10.2136/sssaj1982.03615995004600010013x.

Simarmata, T., Benckiser, G., Ottow, J.C.G., 1993. Effect of an increasing carbon: nitrate-N ratio on the reliability of acetylene in blocking the N_2O-reductase activity of denitrifying bacteria in soil. Biology and Fertility of Soils 15, 107–112. https://doi.org/10.1007/BF00336427.

Spott, O., Russow, R., Apelt, B., Stange, C.F., 2006. A ^{15}N-aided artificial atmosphere gas flow technique for online determination of soil N_2 release using the zeolite Köstrolith SX6. Rapid Communications in Mass Spectrometry 20 (22), 3267–3274. https://doi.org/10.1002/rcm.2722.

Spott, O., Stange, C.F., 2007. A new mathematical approach for calculating the contribution of anammox, denitrification and atmosphere to an N_2 mixture based on a ^{15}N tracer technique. Rapid Communications in Mass Spectrometry 21 (14), 2398–2406. https://doi.org/10.1002/rcm.3098.

Spott, O., Stange, C.F., 2011a. Formation of hybrid N_2O in a suspended soil due to co-denitrification of NH_2OH. Journal of Plant Nutrition and Soil Science 174 (4), 554–567. https://doi.org/10.1002/jpln.201000200.

Spott, O., Russow, R., Stange, C.F., 2011b. Formation of hybrid N_2O and hybrid N_2 due to codenitrification: first review of a barely considered process of microbially mediated N-nitrosation. Soil Biology and Biochemistry 43 (Issue 10), 1995–2011. https://doi.org/10.1016/j.soilbio.2011.06.014.

Stevens, R.J., Laughlin, R.J., Atkins, G.J., Prosser, S.J., 1993. Automated determination of nitrogen-15-labeled dinitrogen and nitrous oxide by mass spectrometry. Soil Science Society of America Journal 57 (4), 981–988. https://doi.org/10.2136/sssaj1993.03615995005700040017x.

Stevens, R.J., Laughlin, R.J., Burns, L.C., Arah, J.R.M., Hood, R.C., 1997. Measuring the contributions of nitrification and denitrification to the flux of nitrous oxide from soil. Soil Biology and Biochemistry 29 (Issue 2), 139–151. https://doi.org/10.1016/S0038-0717(96)00303-3.

Stevens, R.J., Laughlin, R.J., 2001. Lowering the detection limit for dinitrogen using the enrichment of nitrous oxide. Soil Biology and Biochemistry 33 (Issue 9), 1287–1289. https://doi.org/10.1016/S0038-0717(01)00036-0.

Stevens, R.J., Laughlin, R.J., 2002. Cattle slurry applied before fertilizer nitrate lowers nitrous oxide and dinitrogen emissions. Soil Science Society of America Journal 66 (6), 647–652. https://doi.org/10.2136/sssaj2002.6470.

Tanimoto, T., Hatano, K.-I., Kim, D.H., Uchiyarna, H., Shoun, H., 1992. Co-denitrification by the denitrifying system of the fungus Fusarium oxysporum. FEMS Microbiology Letters 93, 177–180. https://doi.org/10.1111/j.1574-6968.1992.tb05086.x.

Tauchnitz, N., Spott, O., Russow, R., Bernsdorf, S., Glaser, B., Meissner, R., 2015. Release of nitrous oxide and dinitrogen from a transition bog under drained and rewetted conditions due to denitrification: results from a [^{15}N]nitrate–bromide double-tracer study. Isotopes in Environmental and Health Studies 51 (2), 300–321. https://doi.org/10.1080/10256016.2015.1011634.

Thamdrup, B., Dalsgaard, T., 2002. Production of N_2 through anaerobic ammonium oxidation coupled to nitrate reduction in marine sediments. Applied and Environmental Microbiology 68 (3), 1312–1318. https://doi.org/10.1128/AEM.68.3.1312-1318.2002.

Vanden Heuvel, R.M., Mulvaney, R.L., Hoeft, R.G., 1988. Evaluation of nitrogen-15 tracer techniques for direct measurement of denitrification in soil: II. Simulation studies. Soil Science Society of America Journal 52 (5), 1322–1326. https://doi.org/10.2136/sssaj1988.03615995005200050021x.

Wagner, S.W., Reicosky, D.C., Alessi, R.S., 1997. Regression models for calculating gas fluxes measured with a closed chamber. Agronomy Journal 89 (2), 279–284. https://doi.org/10.2134/agronj1997.00021962008900020021x.

Wang, R., Feng, Q., Liao, T., Zheng, X., Butterbach-Bahl, K., Zhang, W., Jin, C., 2013. Effects of nitrate concentration on the denitrification potential of a calcic cambisol and its fractions of N_2, N_2O and NO. Plant and Soil 363 (1–2), 175–189. https://doi.org/10.1007/s11104-012-1264-x.

Warner, D.I., Scheer, C., Friedl, J., Rowlings, D.W., Brunk, C., Grace, P.R., 2019. Mobile continuous-flow isotope-ratio mass spectrometer system for automated measurements of N_2 and N_2O fluxes in fertilized cropping systems. Scientific Reports 9 (1), 11097. https://doi.org/10.1038/s41598-019-47451-7.

Well, R., Becker, K.-W., Meyer, B., Langel, R., Reineking, A., 1998. Continuous flow equilibration for mass spectrometric analysis of dinitrogen emissions. Soil Science

Society of America Journal 62 (4), 906–910. https://doi.org/10.2136/sssaj1998.03615995006200040008x.

Well, R., Butterbach-Bahl, K., 2013. Comments on "A test of a field-based ^{15}N-nitrous oxide pool dilution technique to measure gross N_2O production in soil" by Yang et al, 2011 Global Change Biology 17, 3577–3588. https://doi.org/10.1111/gcb.12005. In Global Change Biology (Vol. 19, Issue 1, pp. 133–135.

Well, R., Burkart, S., Giesemann, A., Grosz, B., Köster, J.R., Lewicka-Szczebak, D., 2019a. Improvement of the ^{15}N gas flux method for in situ measurement of soil denitrification and its product stoichiometry. Rapid Communications in Mass Spectrometry 33 (5), 437–448. https://doi.org/10.1002/rcm.8363.

Well, R., Maier, M., Lewicka-Szczebak, D., Köster, J.R., Ruoss, N., 2019b. Underestimation of denitrification rates from field application of the ^{15}N gas flux method and its correction by gas diffusion modelling. Biogeosciences 16 (10), 2233–2246. https://doi.org/10.5194/bg-16-2233-2019.

Wijler, J., Delwiche, C.C., 1954. Investigations on the denitrifying process in soil. Plant and Soil 5 (2), 155–169. https://doi.org/10.1007/BF01343848.

Wrage, N., Velthof, G.L., van Beusichem, M.L., Oenema, O., 2001. Role of nitrifier denitrification in the production of nitrous oxide. Soil Biology and Biochemistry 33 (Issue 12–13), 1723–1732. https://doi.org/10.1016/S0038-0717(01)00096-7.

Wu, H., Dannenmann, M., Fanselow, N., Wolf, B., Yao, Z., Wu, X., Brüggemann, N., Zheng, X., Han, X., Dittert, K., Butterbach-Bahl, K., 2011. Feedback of grazing on gross rates of N mineralization and inorganic N partitioning in steppe soils of Inner Mongolia. Plant and Soil 340 (1), 127–139. https://doi.org/10.1007/s11104-010-0575-z.

Xi, D., Fang, Y., Zhu, W., 2022. Spatial variations of soil N_2 and N_2O emissions from a temperate forest: quantified by the in situ ^{15}N labeling method. Forests 13 (9). https://doi.org/10.3390/f13091347.

Yang, W.H., Teh, Y.A., Silver, W.L., 2011. A test of a field-based ^{15}N-nitrous oxide pool dilution technique to measure gross N_2O production in soil. Global Change Biology 17 (12), 3577–3588. https://doi.org/10.1111/j.1365-2486.2011.02481.x.

Yang, W.H., McDowell, A.C., Brooks, P.D., Silver, W.L., 2014. New high precision approach for measuring ^{15}N-N_2 gas fluxes from terrestrial ecosystems. Soil Biology and Biochemistry 69, 234–241. https://doi.org/10.1016/j.soilbio.2013.11.009.

Yeung, L.Y., Li, S., Kohl, I.E., Haslun, J.A., Ostrom, N.E., Hu, H., Fischer, T.P., Schauble, E.A., Young, E.D., 2017. Extreme enrichment in atmospheric ^{15}N^{15}N. Science Advances 3 (11), eaao6741. https://doi.org/10.1126/sciadv.aao6741.

Yeung, L.Y., Haslun, J.A., Ostrom, N.E., Sun, T., Young, E.D., van Kessel, M.A.H.J., Lücker, S., Jetten, M.S.M., 2019. In situ quantification of biological N_2 production using naturally occurring ^{15}N^{15}N. Environmental Science and Technology 53 (9), 5168–5175. https://doi.org/10.1021/acs.est.9b00812.

Yoshida, N., Toyoda, S., 2000. Constraining the atmospheric N_2O budget from intramolecular site preference in N_2O isotopomers. Nature 405 (6784), 330–334. https://doi.org/10.1038/35012558.

Yu, K., Seo, D.C., Delaune, R.D., 2010. Incomplete acetylene inhibition of nitrous oxide reduction in potential denitrification assay as revealed by using ^{15}N-Nitrate tracer. Communications in Soil Science and Plant Analysis 41 (18), 2201–2210. https://doi.org/10.1080/00103624.2010.504800.

Yu, L., Harris, E., Lewicka-Szczebak, D., Barthel, M., Blomberg, M.R.A., Harris, S.J., Johnson, M.S., Lehmann, M.F., Liisberg, J., Müller, C., Ostrom, N.E., Six, J., Toyoda, S., Yoshida, N., Mohn, J., 2020. What can we learn from N_2O isotope data? – Analytics, processes and modelling. Rapid Communications in Mass Spectrometry 34 (20). https://doi.org/10.1002/rcm.8858.

Zaman, M., Heng, L., Müller, C. (Eds.), 2021. Measuring Emission of Agricultural Greenhouse Gases and Developing Mitigation Options Using Nuclear and Related Techniques : Applications of Nuclear Techniques for GHGs. Springer International Publishing. https://doi.org/10.1007/978-3-030-55396-8.

Zhu-Barker, X., Cavazos, A.R., Ostrom, N.E., Horwath, W.R., Glass, J.B., 2015. The importance of abiotic reactions for nitrous oxide production. Biogeochemistry 126 (3), 251–267. https://doi.org/10.1007/s10533-015-0166-4.

Zou, Y., Hirono, Y., Yanai, Y., Hattori, S., Toyoda, S., Yoshida, N., 2014. Isotopomer analysis of nitrous oxide accumulated in soil cultivated with tea (Camellia sinensis) in Shizuoka, central Japan. Soil Biology and Biochemistry 77, 276–291. https://doi.org/10.1016/j.soilbio.2014.06.016.